

**IMPLEMENTATION OF TORQUE HYSTERESIS CONTROLLER (THC) FOR  
BRUSHLESS DIRECT CURRENT (BLDC) MOTOR**

**NABILAH 'AISYAH BINTI MANSOR**

   
A report submitted in partial fulfilment of the requirements for the degree of  
Bachelor of Electrical Engineering with Honours

اونيورسيتي تيكنيكل مليسيا ملاك  
UNIVERSITI TEKNIKAL MALAYSIA MELAKA

**Faculty of Electrical Engineering**

**UNIVERSITI TEKNIKAL MALAYSIA MELAKA**

**2019**

“I hereby declare that I have read through this report entitle “Implementation of Torque Hysteresis Controller (THC) for Brushless Direct Current (BLDC) Motor” and found that it complies the partial fulfillment for awarding the degree of Bachelor of Electrical Engineering with Honours”

Signature  .....

Supervisor's Name : Dr. Auzani Bin Jidin

Date : 21/6/2019



اونيورسيتي تيكنيكل مليسيا ملاك

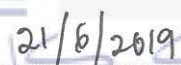
---

UNIVERSITI TEKNIKAL MALAYSIA MELAKA

I declare that this report entitles “*Implementation of Torque Hysteresis Controller (THC) for Brushless Direct Current (BLDC) Motor*” is the result of my own research except as cited in the references. The report has not been accepted for any degree and is not concurrently submitted in candidature of any other degree.

Signature :  .....

Name : NABILAH AISYAH BINTI MANSOR

Date :  .....

UNIVERSITI TEKNIKAL MALAYSIA MELAKA

## DEDICATIONS

To my beloved mother and father

My beloved husband and daughter

My beloved siblings

My beloved supervisor and lecturers

My fellow friends

For their moral support and encouragement through my journey of education



## ACKNOWLEDGEMENT

First and foremost, I would like to express my gratitude to the Almighty Allah SWT for His willing in giving me the strength to complete my Final Year Project 1.

I would love to express my profound gratitude to my supervisor, Dr. Auzani bin Jidin for his exemplary guidance in supervising me throughout the course of this project.

A special thanks to my fellow friends for sharing valuable information along the progress of work as well as my panel 1, Prof. Madya Dr. Kasrul bin Abdul Karim for his time in evaluating my report and giving some opinions during presentation day.

Last but not least, thanks to my husband, my daughter and my both side of family for their moral support and encouragement in completing this project.

اونيورسيتي تيكنيكل مليسيا ملاك

UNIVERSITI TEKNIKAL MALAYSIA MELAKA

## ABSTRACT

This project is about the implementation of Torque Hysteresis Controller of Brushless Direct Current (BLDC) Motor. BLDC motor is well-known and has been widely used in the industrial area due to its high speed and power density capabilities. Electronic commutation is by far more favorable compared to the conventional method, which uses brushes and commutators, that wear and tear by time. However, a precise controller is required in order to control the switches prior to commutation process. Over the past years, Torque Hysteresis Controller (THC) method for induction motor drives received lots of attention from researchers, and motor drive industries. THC of BLDC combines a simple control method and a demanded from BLDC motor to complete a better performance. THC method is known to have a simple structure without having complex calculations thus offers a fast response and a good dynamic performance. The previous work which is the Voltage Controlled of BLDC motor contributes a very high current during the start-up. Furthermore, the conventional implementation gives large ripple with uncontrollable in the restricted bandwidth of hysteresis. A mathematical modeling which is created using Matlab/Simulink simulation on the motor drive for Brushless DC Motor is presented along with a complete model of the THC system for BLDC motor using Simulink Block. Finally, the simulation and are shown to validate the performance of THC of BLDC motor with improvements of the problem highlighted.

## ABSTRAK

Projek ini adalah mengenai pelaksanaan Pengawal Hysteresis Torque Brushless Direct Current (BLDC) motor. Motor BLDC terkenal dan telah digunakan secara meluas di kawasan perindustrian kerana keupayaan berkempen dan kelajuan tinggi. Pergantungan elektronik jauh lebih menguntungkan berbanding dengan kaedah konvensional, yang menggunakan berus dan komutator, yang memakai dan lusuh mengikut masa. Walau bagaimanapun, pengawal tepat diperlukan untuk mengawal suis sebelum proses penggantian. Sepanjang tahun yang lalu, kaedah Pengawasan Torque Hysteresis (THC) untuk pemacu motor induksi menerima banyak perhatian daripada penyelidik, dan industri memandu motor. THC BLDC menggabungkan kaedah kawalan mudah dan menuntut dari motor BLDC untuk menyelesaikan prestasi yang lebih baik. Kaedah THC diketahui mempunyai struktur mudah tanpa pengiraan yang kompleks dengan itu menawarkan tindak balas yang cepat dan prestasi dinamik yang baik. Kerja sebelumnya yang Pengalawan Voltan motor BLDC menyumbang arus yang sangat tinggi semasa permulaan. Selain itu, pelaksanaan konvensional memberikan riak besar dengan tak terkawal dalam jalur lebar hysteresis yang terhad. Pemodelan matematik yang dicipta menggunakan Matlab / Simulink simulasi pada pemacu motor untuk Brushless DC Motor dibentangkan bersama model lengkap sistem THC untuk BLDC menggunakan blok Simulink. Akhir sekali, simulasi dan ditunjukkan untuk mengesahkan prestasi THC motor BLDC dengan penambahbaikan masalah yang diketengahkan.

## TABLE OF CONTENTS

CHAPTER	TITLE	PAGE
	<b>SUPERVISOR'S APPROVAL</b>	<b>i</b>
	<b>TITLE PAGE</b>	<b>ii</b>
	<b>DECLARATION</b>	<b>iii</b>
	<b>DEDICATION</b>	<b>iv</b>
	<b>ACKNOWLEDGEMENT</b>	<b>v</b>
	<b>ABSTRACT</b>	<b>vi</b>
	<b>ABSTRAK</b>	<b>vii</b>
	<b>TABLE OF CONTENTS</b>	<b>viii</b>
	<b>LIST OF TABLES</b>	<b>xi</b>
	<b>LIST OF FIGURES</b>	<b>xii</b>
	<b>LIST OF ABBREVIATIONS</b>	<b>xiv</b>
	<b>LIST OF APPENDICES</b>	<b>xv</b>
<b>1</b>	<b>INTRODUCTION</b>	<b>1</b>
	1.1 Project Background	1
	1.2 Motivation	2
	1.3 Problem Statement	3
	1.4 Objective	3
	1.5 Scope of Research	4
	1.6 Research Methodology	5
<b>2</b>	<b>LITERATURE REVIEW</b>	<b>6</b>
	2.1 Introduction	6
	2.2 Magnetic Force	6
	2.3 Principle Operation of BLDC Motor	7
	2.3.1 Construction of BLDC motor	7



	2.3.2	Operation of BLDC motor with Hall Effect Sensor	15
	2.4	Related Previous Work	17
	2.4.1	Voltage Controlled	17
	2.4.2	Conventional Implementation of Torque Hysteresis Controller of BLDC Motor	20
<b>3</b>		<b>METHODOLOGY</b>	<b>23</b>
	3.1	Introduction	23
	3.2	Mathematical Modelling of BLDC Motor	23
	3.3	Voltage Source Inverter (VSI)	27
	3.4	Principle Operation of THC	28
	3.4.1	Hysteresis Operation	29
	3.4.2	Topology Circuit	31
	3.5	Simulation Model of THC	32
	3.5.1	Simulation Model for Conventional Implementation of THC	32
	3.5.2	Simulation Model for Proposed Method of Torque Hysteresis Controller	35
	3.6	Experimental Setup	38
	3.5.1	Conventional Implementation using dSPACE 1104	38
	3.5.2	Proposed Experimental Setup	39
<b>4</b>		<b>RESULTS AND DISCUSSION</b>	<b>47</b>
	4.1	Introduction	47
	4.2	Parameters Setting for Simulation Proposed THC Technique for BLDC Motor	47
	4.3	Simulation Results	48
	4.3.1	Conventional Implementation of THC	48

	4.3.2	Proposed Method of THC	49
	4.4	Experimental Setup	52
	4.4.1	Conventional Implementation	52
	4.4.2	Proposed Method	55
5		<b>CONCLUSION</b>	<b>58</b>
	5.1	Conclusion	58
	5.2	Future Work	58
		<b>REFERENCES</b>	<b>59</b>
		<b>APPENDICES</b>	<b>61</b>



اونيورسيتي تيكنيكل مليسيا ملاك

UNIVERSITI TEKNIKAL MALAYSIA MELAKA

## LIST OF TABLES

TABLE	TITLE	PAGE
2.0	Hall Sensor with Switching State	18
3.0	Derivation of Decoded Signals based on Hall Effect Signals	32
3.1	Hall Effect Sensor and Incremental Encoder Table	34
3.2	Hall Effect Sensor, Current and Switching State Table	35
4.1	Parameters Value for THC of BLDC Motor	48



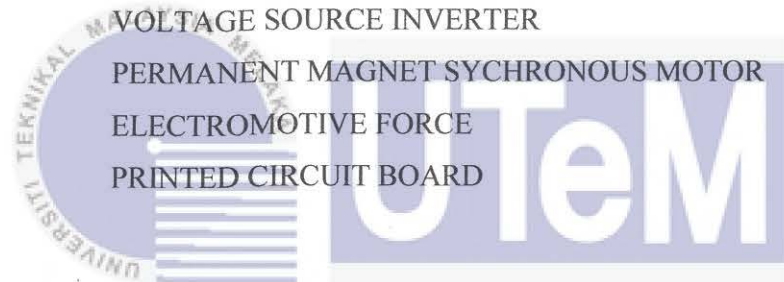
## LIST OF FIGURES

FIGURE	TITLE	PAGE
2.1	Magnetic Force	7
2.2	Structure of Brushless DC Motor	8
2.3	Cross Sectional View of Motors	9
2.4	Stator in a BLDC Motor	11
2.5	Slotted and Slotless Stator Motor	11
2.6	Permanent Magnet of Rotor	13
2.7	Rotor in a BLDC motor	13
2.8	Conceptual Drawing for Hall Effect Sensor	14
2.9	Six Steps Commutation Sequence	16
2.10	Output Graph of Hall Effect Sensor in BLDC Motor	17
2.11	Switching Logic Equation	18
2.12	Schematic of Voltage Controlled	19
2.13	Simulation Results Logic Circuit	20
2.14	Structure of THC for BLDC Motor	21
2.15	Schematic Circuit of Basic THC Implementation	22
2.16	Simulation Result Basic THC Implementation	22
3.1	Three phase BLDC Machine Equivalent Circuit and Mechanical Model	26
3.2(a)	Three-Phase Voltage Source Inverter Topology Circuit	27
3.2(b)	Three-Phase Voltage Source Inverter Simplified Circuit	28
3.3	Block Diagram of Hysteresis Current Controller	30
3.4	Output Graph of Hysteresis Current Switching Control	30
3.5	Structure of Torque Hysteresis Controller (THC) for BLDC motor	31
3.6	Simulation of Decoder Circuit	33
3.7	Complete Block Diagram of Simulation Control for BLDC Motor	34

3.8	Logic Circuit for top IGBT of S1	36
3.9	Logic Circuit for bottom IGBT of S4	36
3.10(a)	Switching of IGBT and Current Phases Normal	37
3.10(b)	Switching of IGBT and Current Phases Hall 001	37
3.11	Complete Block Diagram of Proposed Method for BLDC Motor	37
3.12	Experimental Setup for Conventional Implementation	38
3.13	Experimental Setup for Proposed Method	39
3.14	Schematic of Hall Sensor Signal Detector	40
3.15	PCB of Hall Sensor Signal Detector	41
3.16	Schematic of Hysteresis Current Controller	43
3.17	PCB of Hysteresis Current Controller	43
3.18	Schematic of Logic Circuit	44
3.19	PCB of Logic Circuit	45
3.20	Schematic of Current Sensor	46
3.21	PCB of Current Sensor	46
4.1	Schematic Circuit for Conventional Implementation	49
4.2	Simulation results for Conventional Implementation	50
4.3	Schematic Circuit for Proposed Method	51
4.4	Simulation results for Proposed Method	52
4.5	Results for Bandwidth 0.025A	53
4.6	Results for Bandwidth 0.1A	54
4.7	Results for Bandwidth 0.5A	54
4.8	Results for Bandwidth 0.025A	56
4.9	Results for Bandwidth 0.1A	56
4.10	Results for Bandwidth 0.5A	57

## LIST OF ABBREVIATIONS

BLDC	BRUSHLESS DIRECT CURRENT
BDC	BRUSHED DIRECT CURRENT
DC	DIRECT CURRENT
AC	ALTERNATING CURRENT
IC	INTERGRATED CIRCUIT
THC	TORQUE HYSTERESIS CONTROLLER
IGBT	INSULATED GATE BIPOLAR TRANSISTOR
MOSFET	METAL–OXIDE–SEMICONDUCTOR FIELD-EFFECT TRANSISTOR
VSI	VOLTAGE SOURCE INVERTER
PMSM	PERMANENT MAGNET SYCHRONOUS MOTOR
EMF	ELECTROMOTIVE FORCE
PCB	PRINTED CIRCUIT BOARD



اونيورسيتي تيكنيكل مليسيا ملاك

UNIVERSITI TEKNIKAL MALAYSIA MELAKA

**LIST OF APPENDICES**

<b>APPENDIX</b>	<b>TITLE</b>	<b>PAGE</b>
A1	GANTT CHART	61
A2	MILESTONES	61
B	MATLAB SIMULATION FOR DSPACE 1104	62
C	DATA SHEET AD8022	63
D	DATA SHEET SN74S07L	64
E	DATA SHEET ADR381	65
F	DATA SHEET AD8276	66
G	DATA SHEET TLV3201	67



اونيورسيتي تيكنيكل مليسيا ملاك

UNIVERSITI TEKNIKAL MALAYSIA MELAKA

## CHAPTER 1

### INTRODUCTION

#### 1.1 Project Background

Conventional Direct Current motors are exceptionally effective and their trademark makes it reliable for use in numerous applications. In any case, there are some disadvantages in this motor since it's using a commutator and brushes which needs maintenance frequently and besides it's can't be performed at dirty and hazardous condition also in faster working conditions [8]. Thus, machine with maintenance free can be created by replacing the elements of commutator and brushes by strong state switches, and these sorts of engines are currently known as Brushless Direct Current Motors (BLDC). In fact, (BLDC) is a type of permanent magnet synchronous motors (PMSM). The current commutation is done by solid-state switches and it's supplied by DC voltage.

BLDC Motor has an advantages such as fast torque response besides capable in high speeds drive compared with DC Motor for longer lifespan [6]. Placement of coils in the stator and permanent magnet in the rotor are the basic operating principles of DC motor operation used in BLDC motor. Winding of coils are electrically separated from each other, where creates a rotating magnetic field by allowing it turn on and off in a sequence. The position of rotor needs to be determined, as so the stator fields' excitation always leads to produce a torque by permanent magnet field. Rotor position which later



determine the commutation instants and it is also detected either by sensor less techniques or position of sensors BLDC Motor need to be decoded by the signal from the Hall Effect Sensor then can determine the shaft and energize the appropriate windings of stator [5].

Operation of BLDC motor necessary needs the power electronic converter. BLDC motor consists of three phases DC to AC converter with a six solid-state semiconductor switches. The most common used type of switches was MOSFET and IGBT. In low power applications, MOSFET is preferable compared to IGBT. Positive, negative and zero voltage should be applied by the power electronic inverter to the terminals phase of motor. Each phase contains of high, low and floating terminals.

## 1.2 Motivation

As known in many applications, Direct Current (DC) motors proven in their efficiency and reliable characteristics besides it can be operated at fixed speed in a fixed voltage compared with an AC motors. Furthermore, conventional DC motors such as Brushed DC motor (BDC) have many disadvantages especially on their mechanical parts. Brush and commutator needed in order to operate BDC motor which later limit its capability. Therefore, to overcome the problem, BLDC motor is proposed. In the view of controlling mechanism, BLDC motors has a good speed control compared to conventional methods. One of the control method named Voltage Controlled of BLDC motor. The main problem by using Voltage Controlled method for BLDC motor is the uncontrollable in measurement of current during start-up. Thus, the Torque Hysteresis Controller (THC) of BLDC motor is introduced due to its advantages to overcome the problem on previous work.

### 1.3 Problem Statement

The basic control method for BLDC motor is Voltage Controlled method. But somehow this method having some drawbacks which need to overcome for a better performance on BLDC motor. The main problem is this method has a poor torque and current dynamic control where its produce inrush current during start-up besides it also doesn't provide a current limitation in this method. The torque and speed increases whenever there is a large demand given due to no current control. In this method, there is no current sensor been used and hall effect sensor signal; is the only feedback that they have been used to run the method. Besides, with conventional method of THC, the torque and current ripple become larger and uncontrollable.

### 1.4 Objective

The purposes of this project are to:

1. To produce excellent torque dynamic control using hysteresis controllers for BLDC Motor.
2. To develop/implement of Torque Hysteresis Controller (THC) of BLDC Motor using Analogue Integrated Circuit (ICs).
3. To evaluate the improvements, i.e. excellent torque/current using Analogue ICs through simulation/experiment results.

## 1.5 Scope of Research

This project mainly focuses on:

1. Understand the behavior and operation of BLDC Motor.
  - At this stage, it is necessary to know the construction of BLDC Motor and the mathematical modelling of BLDC Motor.
2. Study various control techniques of BLDC Motor.
  - Various techniques that need to study such as Voltage Controlled, Direct Torque Current (DTC) and Torque Hysteresis Controller (THC).
  - Understand THC operation for BLDC Motor.
3. Develop simulation model of THC for BLDC Motor
  - Develop simulation model by using Matlab/Simulink for Voltage Controlled and Digital Implementation of THC.
  - Develop simulation model for proposed method which is fully using Analogue ICs by using Matlab/Simulink.
4. Implement the hardware system for THC of BLDC Motor
  - Identify the components/devices which are suitable for this research.
  - Design Printed Circuit Board (PCB) Layout by using Orcad Pspice.
5. Evaluate the improvements of the proposed method.
  - Evaluate comparison between torque/current of digital and analogue ICs.

## 1.6 Research Methodology

First and foremost, the behavior and operation of BLDC Motor needs to understand to ensure the research to run smoothly. Besides, understanding about the construction of BLDC Motor which consists of Stator, Rotor and Hall Effect Sensor and mathematical modelling of BLDC Motor that will used in simulation in Matlab/Simulink are needed. Furthermore, various control technique of BLDC Motor such as Voltage Controlled and Torque Hysteresis Controller (THC) need to be studied. In this research, torque hysteresis controller (THC) is used and understanding about THC operation for BLDC Motor is more focused. Next, in this research, development of simulation model of THC for BLDC Motor by using Matlab/Simulink for digital and analogue implementation. After that, implement the hardware system by using THC for BLDC Motor. Before implement hardware system, the component or devices that are suitable in the research need to identify. Printed Circuit Board (PCB) Layout is designed using Orcad Pspice Software. Last but not least, evaluate the improvement of the proposed method which is Torque Hysteresis Controller (THC). Grant Chart which describe the research or activities on planning is given in Appendix A.

## CHAPTER 2

### LITERATURE REVIEW

#### 2.1 Introduction

This chapter is discussing about literature review so as to realize enough data which will be used to complete the analysis. All the data in this chapter are taken from thesis, books, journals, and any educational articles that are associated with the analysis topic and can be clearly cited. Information about THC of BLDC is also highlighted in order to identify the problem occur in the THC itself. Theoretical of magnetic force and basic principle operation of BLDC are explained well. This section reviews about simulation of method between the Voltage Controlled and Implementation of Basic THC for Brushless Dc Motor. Both methods are briefly explained and the problem of each method are mentioned.

#### 2.2 Magnetic Force Theory

Invisible lines of magnetic force generate by magnetic poles flowing from North to South Pole as shown in Figure 1. When magnetic poles of opposite polarity face each other, they generate an attractive force, while like poles generate a repulsive force. [9]

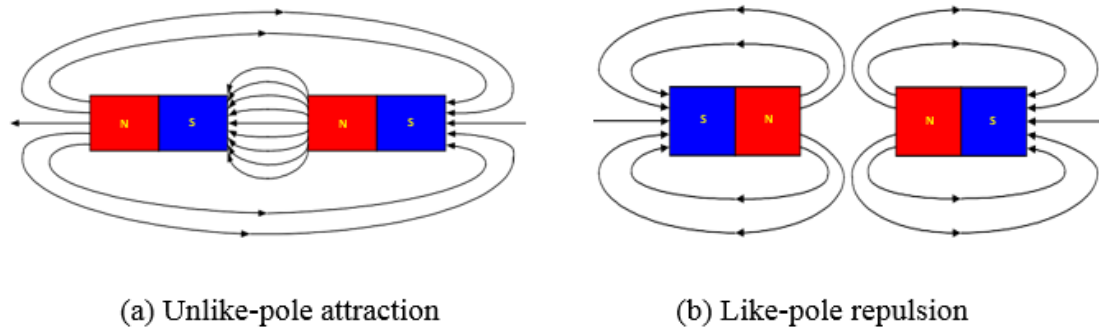


Figure 2.1: Magnetic Force

### 2.3 Principle Operation of BLDC Motor

This section is about principle operation of Brushless Direct Current (BLDC) Motor. Detailed explanation on construction of BLDC Motor which consist of Stator, Rotor and Hall Effect Sensor. Furthermore, operation of BLDC Motor with Hall Effect Sensor is also explained well in this section.

#### 2.3.1 Construction of BLDC Motor

In order to make the operation more reliable or more efficient and less noisy, in recently trends has been use the brushless DC motor; they also lighter compare to brushes motor with the same power output. Basically, BLDC motors used to be high performance motors that also capable to produce large amount of torque with a vast speed range. Figure 2.2 shows structure of BLDC motor while Figure 2.3(a) and Figure 2.3(b) show the cross sectional view DC and BLDC motors. Both motors are commonly used nowadays that also share the same torque and speed performance curve characteristics.

Compare with brushed DC motor (BDC) system, the brushless DC motor (BLDC) system has a better performance. The present of brush gear and commutator in conventional DC machine reduce the speed operation rather than in BLDC, which leads increases in weight and volume. The advantage of permanent magnet rotor is leads to elimination of rotor copper losses which later improved the thermal characteristics. The diameter of rotor tends to become smaller compared to a conventional brushed motor, since there is a development of high energy permanent magnet. This also gives lower rotor inertia and faster the acceleration.

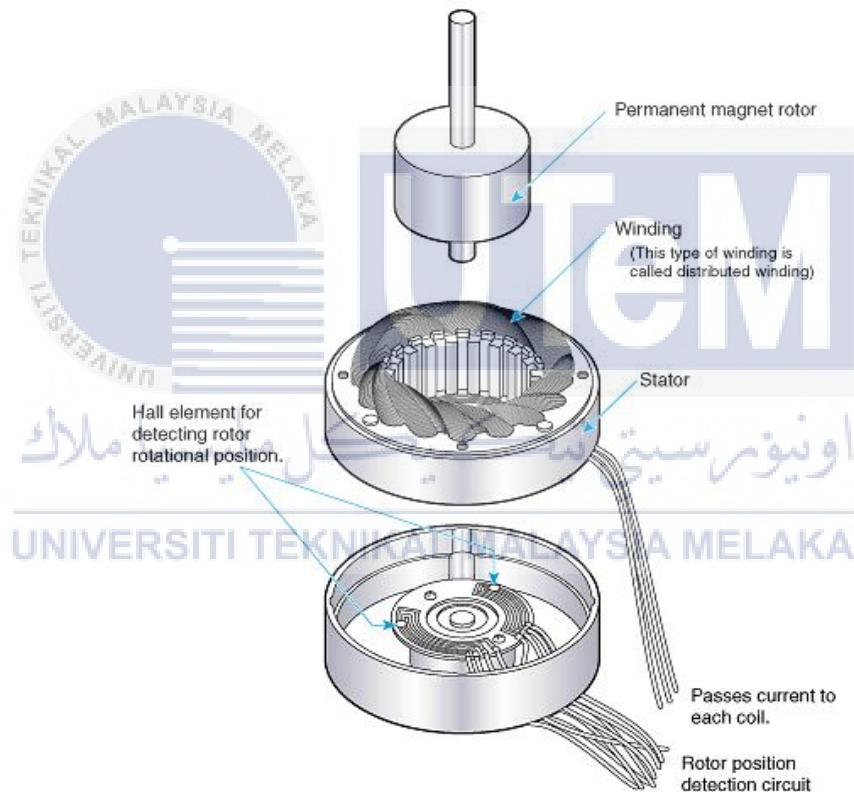


Figure 2.2: Structure of Brushless DC Motor [10]

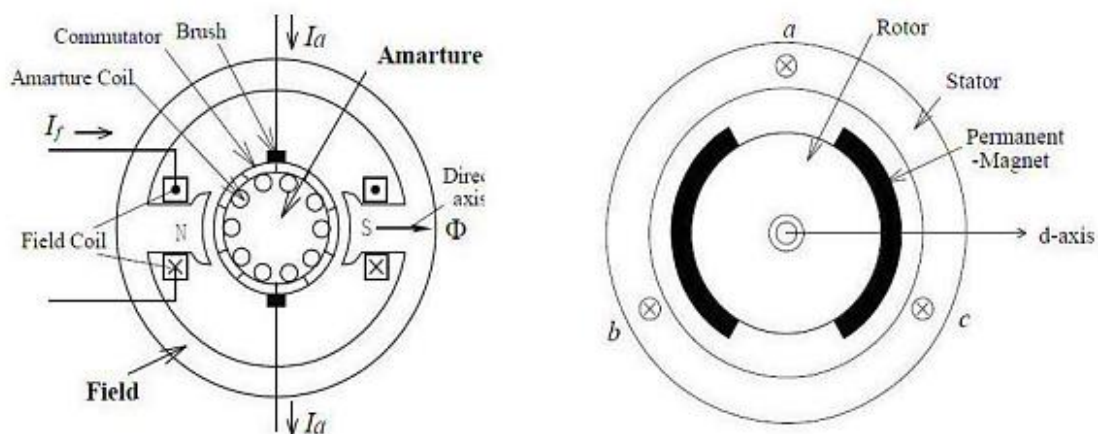


Figure 2.3: Cross Sectional View of Motors

An induction motor has a good property for high speed applications. But, they have low efficiency and power factor when operates at low speed just because of the heavy weight. Furthermore, the construction of it become costly. Different with synchronous motor such as BLDC motor has a better performance for low speed drives since the efficiency of BLDC is higher. Even though the construction of BLDC is more complex, lower weight and cost compared to induction motor gives equal power and speed. The power factor of a plant can be improved by using a synchronous motor together its rated load. Synchronous motor starting torque is larger than an induction motor due to the high resistance of the squirrel-cage winding but not affected the speed and efficiency at synchronous speed. Brushless DC motors usually consist of three main parts which are a Stator, a Rotor and Hall Sensors.



### 2.3.1.1 Stator

Stator of BLDC motor is made up from laminated steel stacked up to carry the windings as shown in Figure 2.4. There are two possible patterns of windings that can be arranged in the stator, i.e. a star pattern (Y) or delta pattern ( $\Delta$ ). The difference between those two patterns is that the Y pattern gives high torque at low speed while the  $\Delta$  pattern gives low torque at low speed. This is because half of the voltage in delta configuration applied across the winding that is not driven, thus increasing losses, efficiency and torque.

Steel laminations in stator can be either slotted or slotless as shown in Figure 2.5(a) and Figure 2.5(b). An advantage of the brushless motor design where the rotor which inside the stator have more cross sectional area for the power or armature winding. At the same time, it is helped to improved time of conduction of heat through the frame. A slotless core can run at very high speed because it has a lower inductance. Besides, the absence of teeth in lamination stack make them an ideal fit for low speed too since it is less requirement for the cogging torque (interaction between aligned permanent magnets on rotor and tooth of stator produce an undesirable cogging torque and create a ripples in speed).

Furthermore, the disadvantage of slotless core is higher cost because it requires more winding to be fit in the larger air gap. Selection on the magnetization of permanent magnets and their displacement on the rotor, so that the shape of back EMF (the voltage induced to the stator winding due to rotor rotation) is trapezoidal. Thus creates rotational field with low torque ripple from a rectangular DC voltage. The motor can have more than one pole-pair per phase. Proper selection on laminated steel and construction of stator windings are important to motor performance. An improper selection may cause multiple problems during producing, marketing delays and high designing costs.



Figure 2.4: Stator in a BLDC Motor

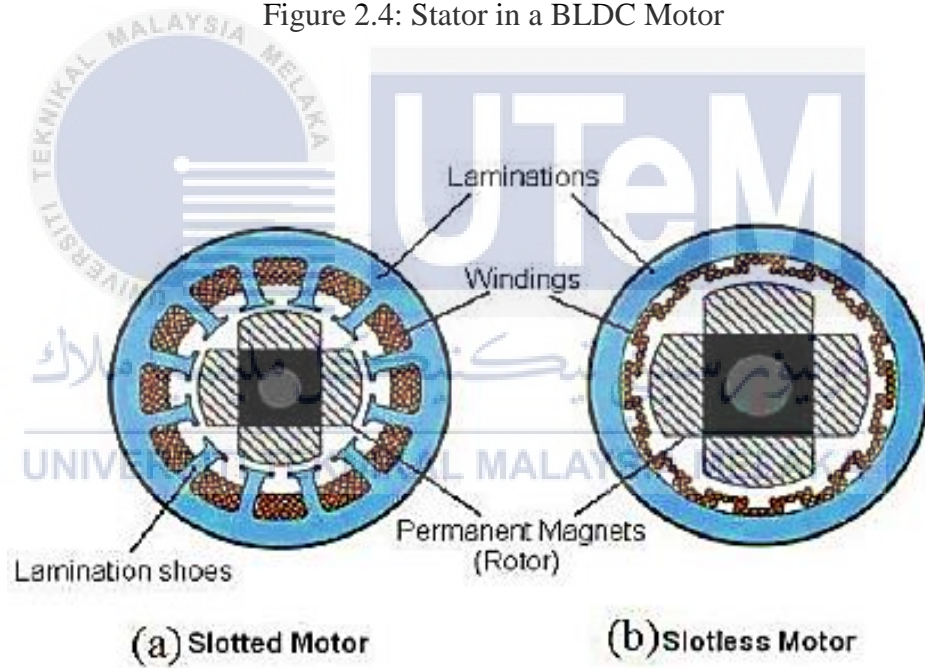


Figure 2.5: Slotted and Slotless Stator Motor [13]

### 2.3.1.2 Rotor

The number of poles in the motor may different depends on the application requirements. Figure 2.6(a) and Figure 2.6(b) show four and eight poles of the permanent magnet rotor respectively. The higher poles number give better torque response but the cost need to be reduced with the maximum possible speed. The material used for the construction of permanent magnet is important since it gives an impact on the maximum torque. The higher the flux density of the material, the higher the torque of motor.

The rotor in a Brushless DC motor contains of an even number of permanent magnets. The number of magnetic pole in rotor affects the step size and torque ripple of the motor. Any of these permanent magnet brushless motor (PMBLM) rotor configurations can be select based on the basic of application and power rating. Due to construction of permanent magnet, the flux density of the rotor is higher lead to no losses occur in the rotor because of no winding present in core. Figure 2.7(a) and Figure 2.7(b) show one and two pair of poles rotor of BLDC motor.

The permanent magnets go from one to five pairs of pole while the rotor can be varying from two to eight pole pairs with North (N) and South (S) poles. The proper magnetic material need to be choose to make a rotor based on the rotors' requirement magnetic field density. Traditionally, ferrite magnet used to make a permanent magnet. But nowadays, with an advanced technology, rare earth alloy magnets become more popular. Ferrite magnets are less expensive but actually they have a disadvantage on low flux density for a certain volume. On other hand, alloy material has high magnetic density per volume and the rotor able to compress further with the same torque. Other than that, alloy magnets also improve the size-to-weight ratio and give higher torque similar with the same size of motor using ferrite magnets.

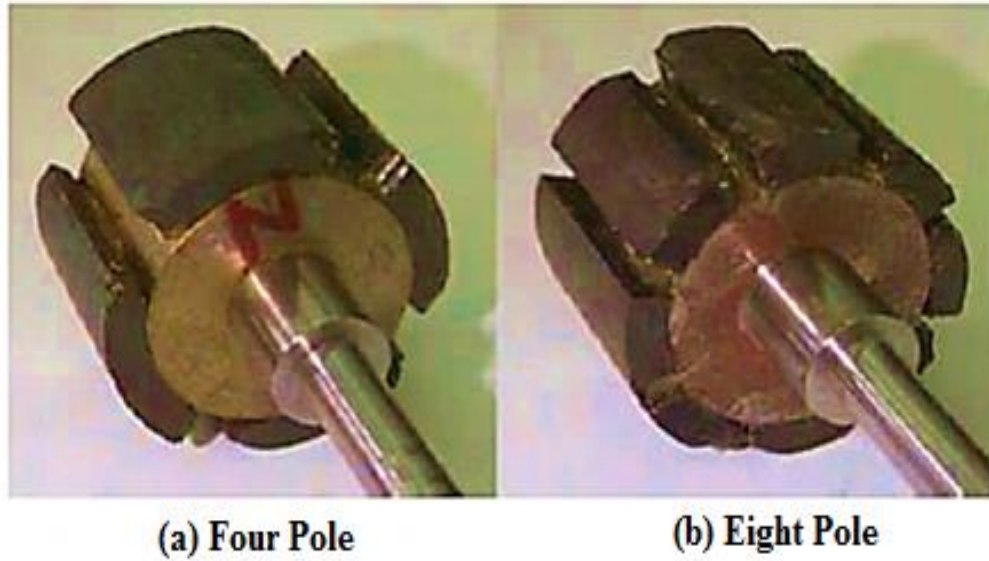


Figure 2.6: Permanent Magnet of Rotor

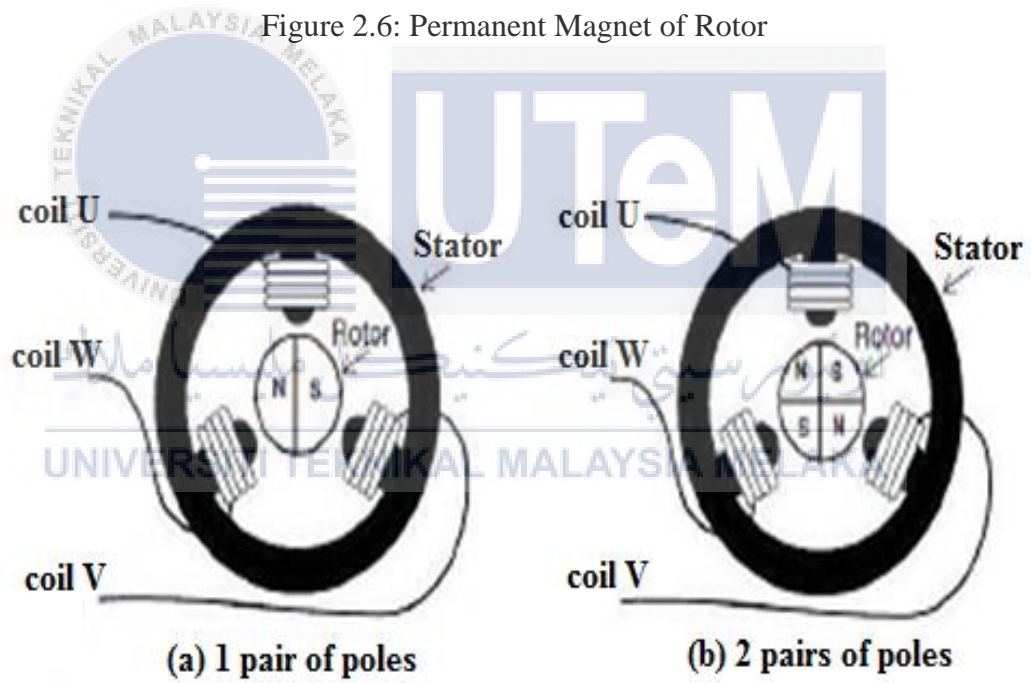


Figure 2.7: Rotor in a BLDC motor

### 2.3.1.3 Hall Effect Sensor

A three phase BLDC motor needs three Hall sensors to detect the position of rotor. There are two types of output which are a  $60^\circ$  phase shift and a  $120^\circ$  phase shift. Both shifts are all based on the physical position of the Hall sensors. Combination of these three Hall sensor signals can identify the exact commutation sequence [2]. Figure 2.8 shows conceptual drawing and three Hall sensors inside a motor. For easy understanding, the stator is shown in simplified form, without its coil windings. The Hall sensors are located at one end of the stator just near to the pole faces of the rotor. Five wires make a connection to the hall sensors. Three wires for individual sensor output while the fourth and fifth wires are for +5Vdc and Ground.

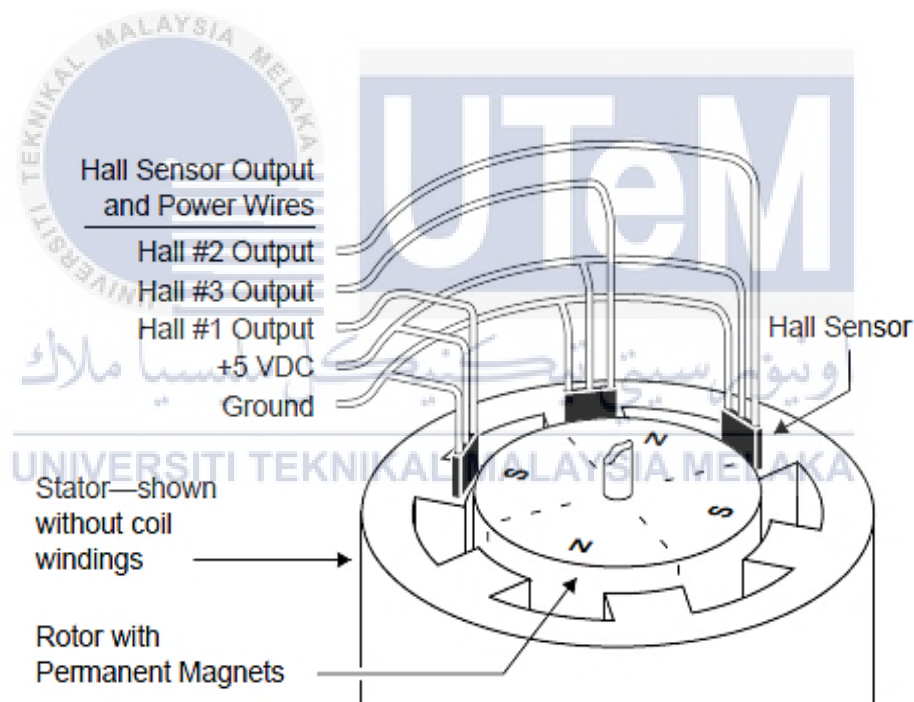


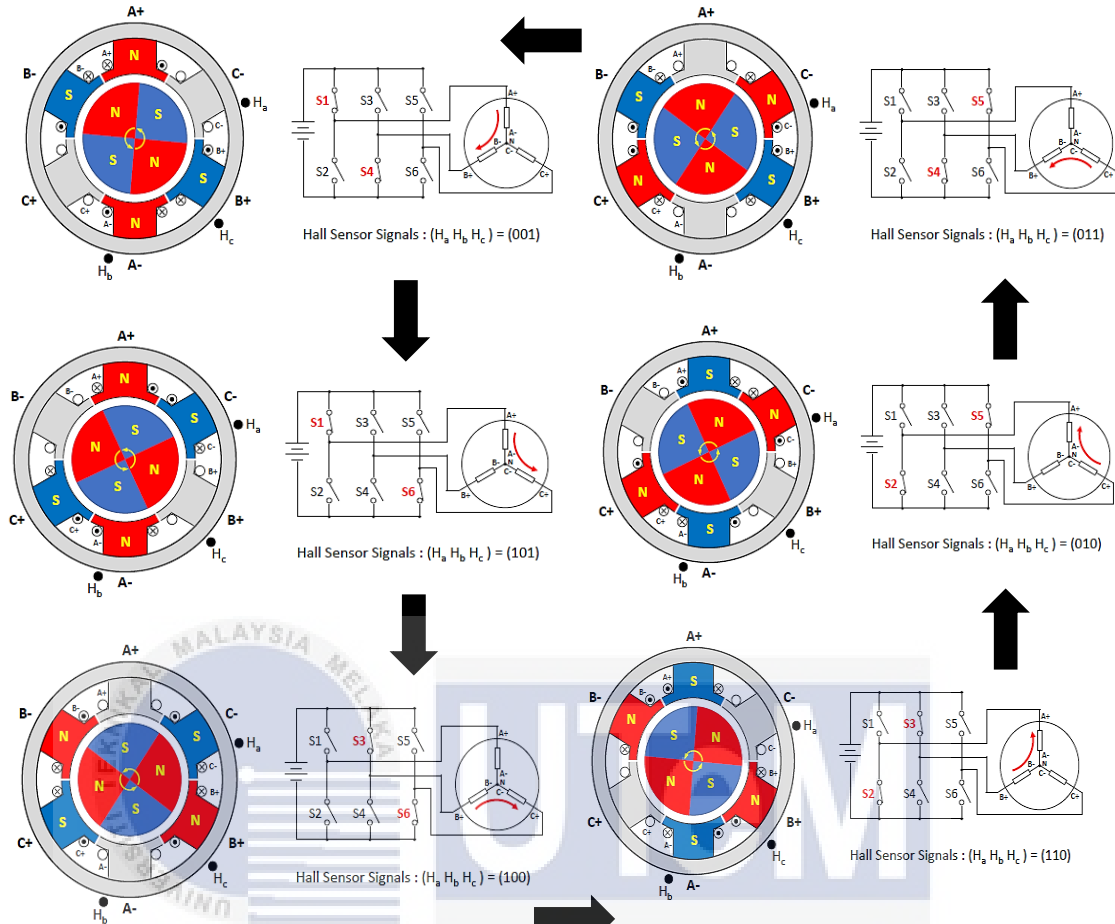
Figure 2.8: Conceptual Drawing for Hall Effect Sensor

### 2.3.2 Operation of BLDC Motor with Hall Effect Sensor

In most BLDC motor control applications, Hall Effect Sensor is used as to determine the rotor position by the position of sensor. Figure 2.9 shows the commutation sequence of a three phase BLDC motor in an anticlockwise rotation. Three Hall sensors, “Ha”, “Hb”, and “Hc” are mounted on the stator at  $120^\circ$  intervals in the electrical part whereas three phase windings are in a star configuration. One of the Hall sensor changes its state in every  $60^\circ$  of rotation and overall takes six steps to complete a whole electrical cycle. That’s means that the phase current switching also updated every  $60^\circ$  in a synchronous mode. There is one motor terminal that driven high, another terminal driven low and the third one floating in each step.

Motor rotates as there is current pass through the windings of the motor. As example, first step in Figure 2.9 shows the current flow from positive to negative (A to B) lead determine by the switching of the inverters where connected to BLDC motor. Next, the current flows determine the winding of the stator either IN or OUT and generates magnetic field from NORTH to SOUTH. Then, North Pole of the stator will align with South Pole in the rotor and vice versa. Meanwhile, same pole will repel each other in order to make the motor rotates. Same concept applied to the next step but with different current flow.

Figure 2.10 shows the timing diagram where the phase winding A, B and C are either in positive, negative or floating state based on the Hall sensor signal Ha, Hb and Hc. This is an example of an anti-clockwise rotation Hall sensor having a  $120^\circ$  phase shift with respect to each other. It is also shows that Hall signal producing different timing sequence when  $60^\circ$  phase shift with an anti-clockwise rotation.



اونیورسیتی تکنیکل ملیسیا ملاک  
 Figure 2.9: Six Steps Commutation Sequence  
 UNIVERSITI TEKNIKAL MALAYSIA MELAKA

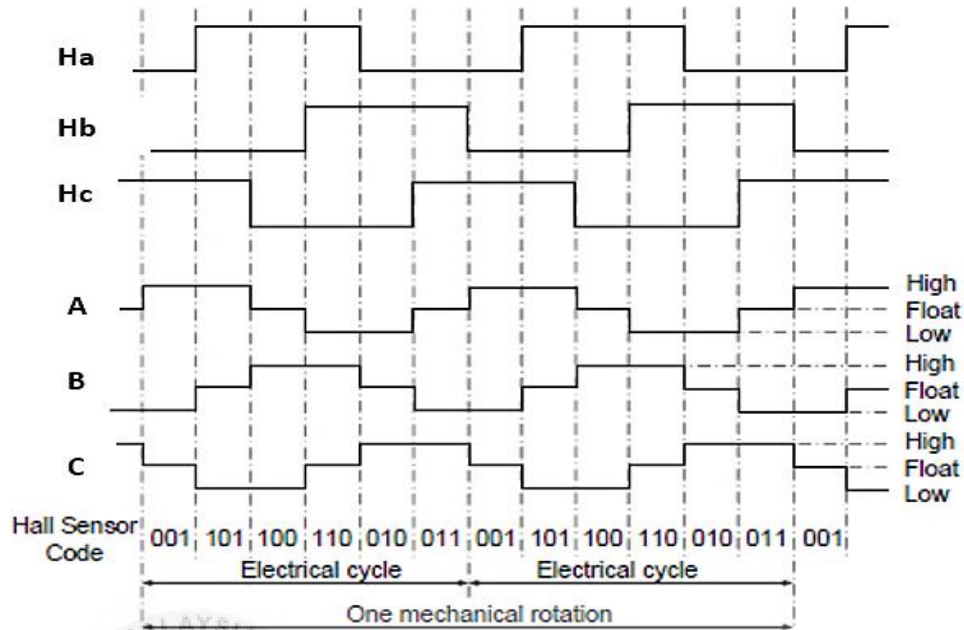


Figure 2.10: Output Graph of Hall Effect Sensor in BLDC Motor

## 2.4 Related Previous Work

This section is about previous work related to switching control for BLDC Motor. There are two methods; Voltage Controlled and Conventional Implementation of Torque Hysteresis Controller (THC). Simulation and result for both methods are shown as well.

### 2.4.1 Method 1: Voltage Controlled

Table 1 shows the Hall sensor signals with its' switching states. Different Hall signals involved different switching state. Logic equation for each switching can be obtained from all the Hall sensor signals and switching state. As example, for switching 1 (S1), the Hall sensor signals are [0 0 1] and [1 0 1]. Ha logic is [0 1]; it cancelled out, Hb logic [0 0]; equal to 0 or **Hb** and Hc logic [1 1]; become 1 or Hc. At the end for S1 = **Hb**



+ Hc. Figure 2.11 shows overall logic equation for all switching state. NOT gate and AND gate are used to combination the switching state involved to produce an equation.

Table 2.0: Hall Sensor with Switching State

<b>Ha</b>	<b>Hb</b>	<b>Hc</b>	<b>S1</b>	<b>S2</b>	<b>S3</b>	<b>S4</b>	<b>S5</b>	<b>S6</b>
0	0	1	1	-	-	1	-	-
1	0	1	1	-	-	-	-	1
1	0	0	-	-	1	-	-	1
1	1	0	-	1	1	-	-	-
0	1	0	-	1	-	-	1	-
0	1	1	-	-	-	1	1	-

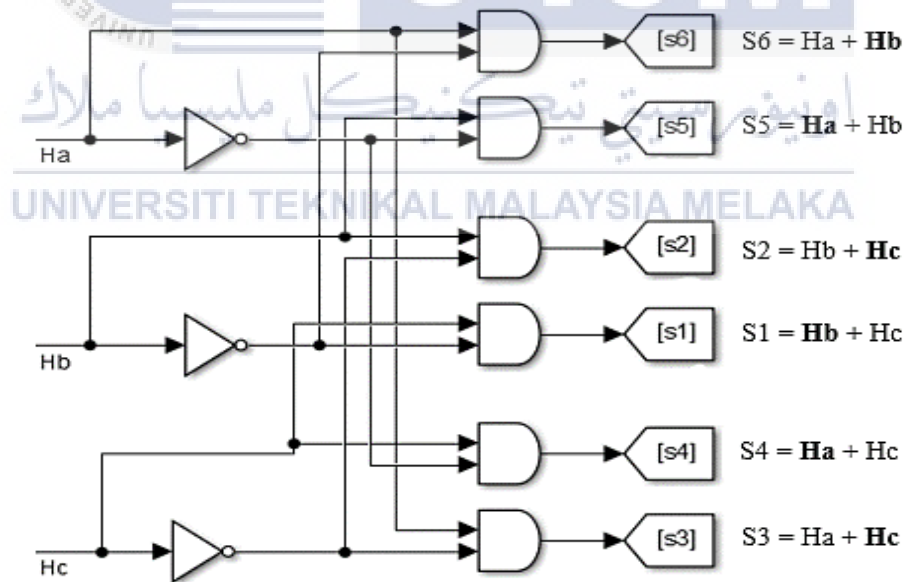


Figure 2.11: Switching Logic Equation

Schematic of Voltage Controlled shown in Figure 2.12 is a combination of switching logic equation, motor parameters and inverter. Since there is no closed loop torque, this basic commutation circuit actually can't control current. Otherwise, the speed can be controlled by adjustment of DC Voltage. Figure 2.13 shows the simulation result of the logic circuit. There are three graphs; speed, torque and current. The step change happens at 0.5s from 12V to 24V, represent using circuit breakers. Some problems detected by using this Voltage Controlled or basic commutation logic circuit. Voltage Controlled of BLDC is using a concept where the speed of motor is directly proportional to voltage supply to motor terminals. The larger the voltage source, the faster the speed of motor. The main problem of this control strategy is poor dynamic response. The response only starts up at 0.2s. Besides, there is an inrush current during start-up of the motor, since it doesn't provide a current limitation and no current sensor used. As the larger demand given, speed of the motor increases as well as the torque and current produced due to no current control. The ripples of torque and current also larger and system become bulky with two circuit breakers to control voltage demand.

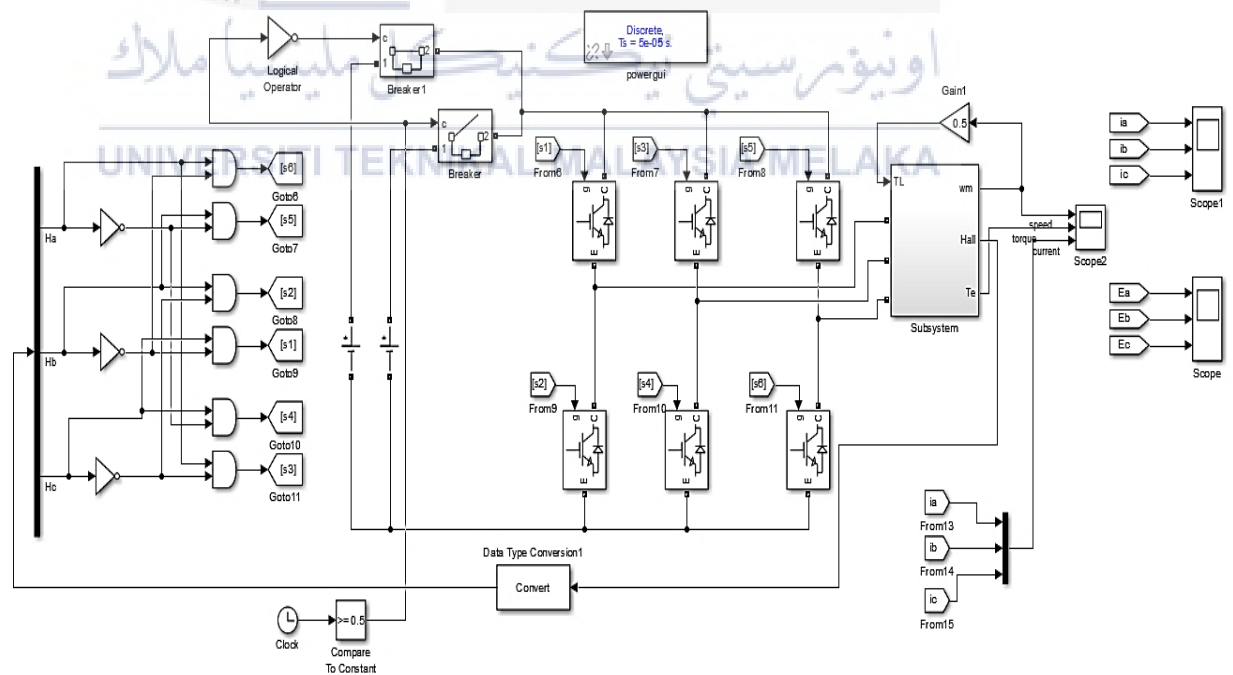


Figure 2.12: Schematic of Voltage Controlled

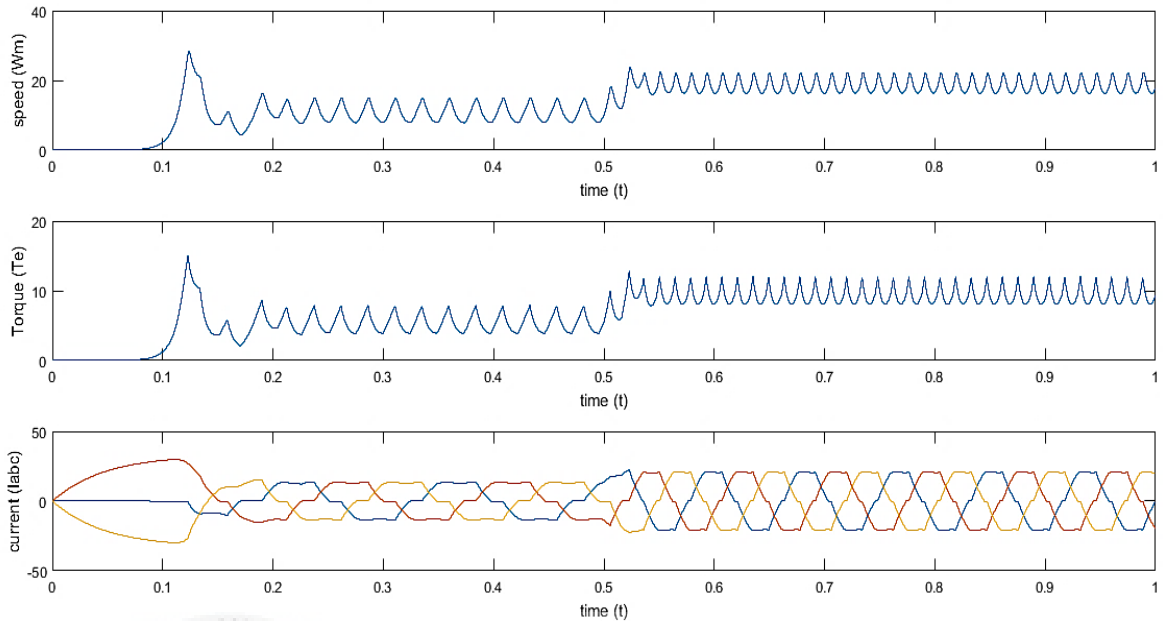


Figure 2.13: Simulation Results Logic Circuit

#### 2.4.2 Method 2: Conventional Implementation of Torque Hysteresis Controller of BLDC Motor

Torque Hysteresis Controller (THC) is a method to replace Voltage Controlled method in order to have a better control in torque and phase current for the BLDC motor. THC able to protect the current, avoid the overshoot current happen in voltage control method. THC is about to control the torque and current restricted in the limit around reference value. Besides, hysteresis control is the simplest closed-loop since the variable that controlled stay within the references. BLDC motor combine with THC can gives an excellent torque dynamic performance. Figure 2.14 shows the structure of THC. The three-phase motor current need to be control followed the reference so as the torque can be control as well. Noted that the total production of torque is given as below.

$$T_{e,total} = T_{e,a} + T_{e,b} + T_{e,c} = k_{t,a}i_a + k_{t,b}i_b + k_{t,c}i_c \quad (2.1)$$

Where  $i_a, i_b, i_c$  = phase current

$k_{t,a}, k_{t,b}, k_{t,c}$  = torque constant (for each phase winding)

Figure 2.14 consists two level hysteresis comparator that used to control current phases as also used to produce proper switching status. The switching status then fed into the inverter, reading of increase or decrease of phases current and the current error ripple stayed in the hysteresis band. Unfortunately, torque hysteresis control with conventional implementation has some disadvantages. Figure 2.15 shows drawn conventional implementation circuit with sampling time of  $50\mu s$ . Due to high sampling time on the conventional implementation, large current and torque ripple are produced as shown in Figure 2.16. Sampling time means that every seconds that set in the system, the production of graph will be different. There is also non-smooth of graph because of the delay action due to large sampling time. Furthermore, with high sampling time, current tend to overshoot out of the hysteresis band and high switching frequency which may lead to high losses in the circuit.

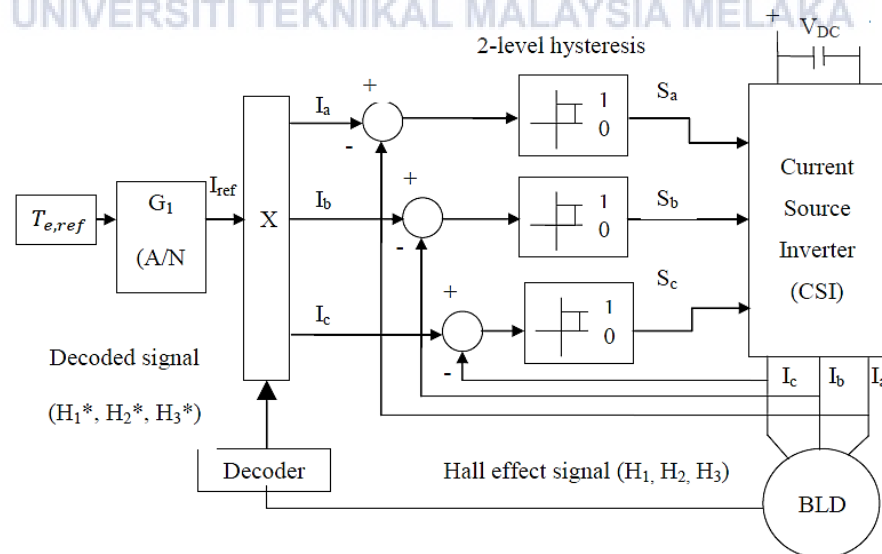


Figure 2.14: Structure of THC for BLDC Motor

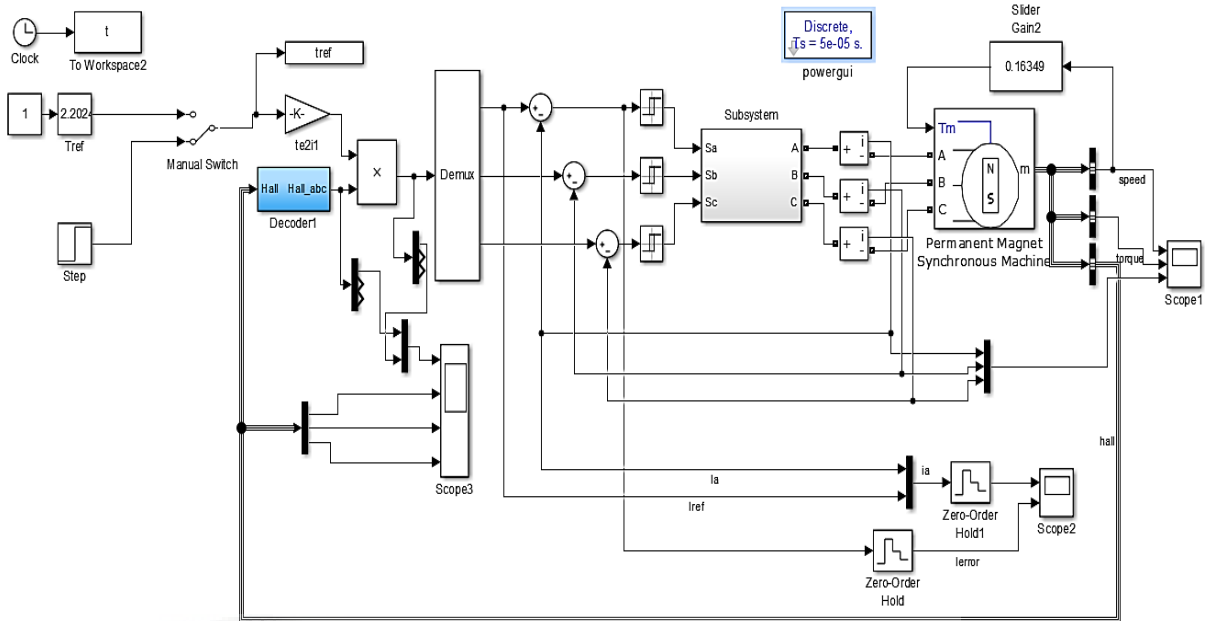


Figure 2.15: Schematic Circuit of Basic THC Implementation

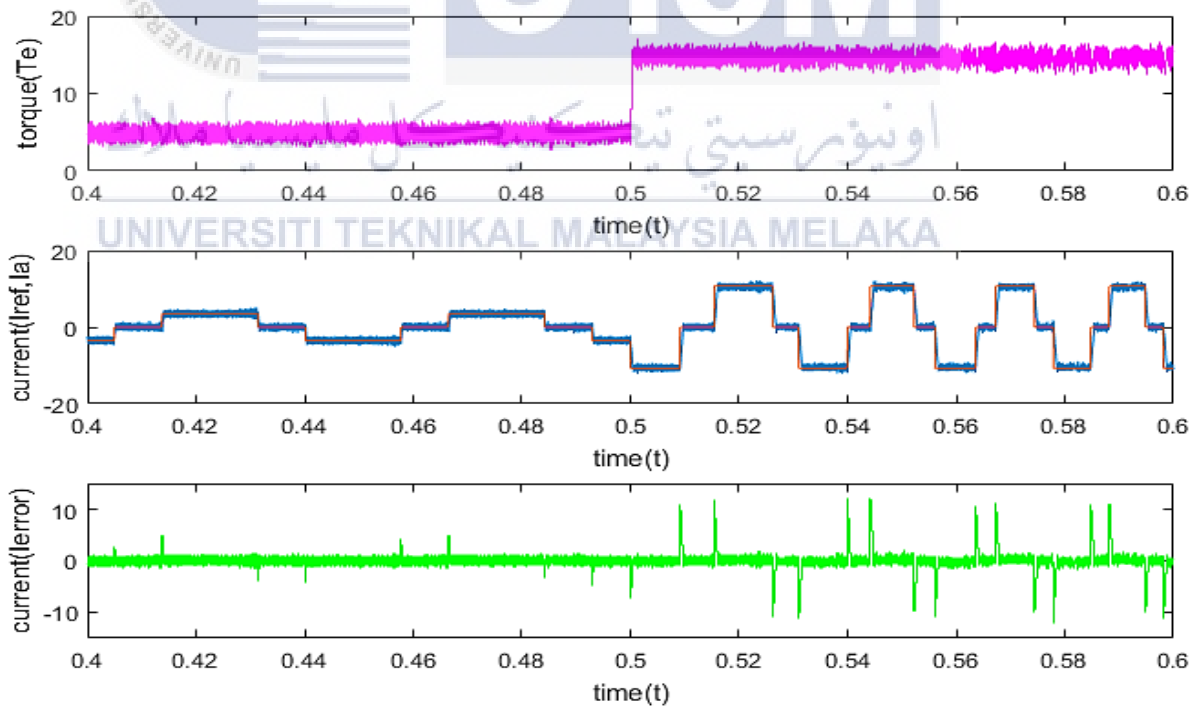


Figure 2.16: Simulation Result Basic THC Implementation

## CHAPTER 3

### METHODOLOGY

#### 3.1 Introduction

Implementation of THC method will be carried out based on the investigation about various control strategy of BLDC motor. First and foremost, to look its' anatomy and the mathematical modeling of BLDC motor. Electrical and mechanical equations are important in order to model BLDC motor. Besides, theoretical on Voltage Source Inverter (VSI) is also explained. Next, research on torque hysteresis controller (THC) is needed to propose new method implementation. This chapter will also give brief explanations on proposed experimental setup with Conventional Implementation of THC by using dSPACE 1104. Last but not least, the proposed experimental setup, totally using analogue ICs presented along with details explanation and schematic circuit of each ICs.

#### 3.2 Mathematical Modelling of BLDC Motor

The basic blocks of BLDC motor shown in Figure 3.1 consists of three-phase stator circuit and part of mechanical. Construction of BLDC motor differ compared to conventional DC motor. BLDC motor contains three-phase windings at the stator with some number of poles. The permanent magnet of rotor centered by the bearing. Non-

electrically rotor connect to the stator to avoid arcing phenomena (production of making an insulation failure). The mathematical model of armature winding is expressed as:

$$V_a = i_a R + L \frac{di_a}{dt} + e_a \quad (3.1)$$

$$V_b = i_b R + L \frac{di_b}{dt} + e_b \quad (3.2)$$

$$V_c = i_c R + L \frac{di_c}{dt} + e_c \quad (3.3)$$

Where  $V_a, V_b, V_c$  = Terminal voltages of phase a, b and c [V]

$i_a, i_b, i_c$  = Stator current of phase a, b and c [A]

$e_a, e_b, e_c$  = Back emf of phase a, b and c [V]

$L$  = Per phase armature self-inductance [H]

$R$  = Per phase armature resistance [ $\Omega$ ]

The back emf are displaced by  $120^\circ$  from one phase to another and is expressed as:

$$e_a = K_e f(\theta_e) \omega_m \quad (3.4)$$

$$e_b = K_e f\left(\theta_e - \frac{2\pi}{3}\right) \omega_m \quad (3.5)$$

$$e_c = K_e f\left(\theta_e + \frac{2\pi}{3}\right) \omega_m \quad (3.6)$$

Where  $\omega_m$  = Mechanical rotor speed [ $\text{rad.s}^{-1}$ ]

$K_e$  = Back emf constant [ $\text{V/rad. s}^{-1}$ ]

$f(\theta_e)$  = Trapezoidal function

$\theta_e$  = Electrical angle of rotor [ $\theta$ ]

Subtract equation (3.2) from (3.1) and (3.3) from (3.2) yield:

$$V_{ab} = R(i_a - i_b) + L \left( \frac{di_a}{dt} - \frac{di_b}{dt} \right) + (e_a - e_b) \quad (3.7)$$

$$V_{bc} = R(i_b - i_c) + L \left( \frac{di_b}{dt} - \frac{di_c}{dt} \right) + (e_b - e_c) \quad (3.8)$$

According to the Kirchoff's Current Law (KCL), the total phase current is equal to zero for wye-connected three-phase winding. Thus, the equation expressed is:

$$\begin{aligned} i_a + i_b + i_c &= 0 \\ i_c &= -i_a - i_b = 0 \end{aligned} \quad (3.9)$$

Substitute  $i_c$  from (3.9) to (3.8):

$$\begin{aligned} V_{bc} &= R(i_b - (-i_a - i_b)) + L \left( \frac{di_b}{dt} - \frac{d(-i_a - i_b)}{dt} \right) + (e_b - e_c) \\ V_{bc} &= R(i_a + 2i_b) + L \left( \frac{di_a}{dt} + 2 \frac{d(i_b)}{dt} \right) + (e_b - e_c) \end{aligned} \quad (3.10)$$

The other equation needs to be considered in modeling BLDC motor is the mechanical equation. In order to describe the machine's angular motion, see Figure 3.1 and Equation 3.11.

$$T_d(t) = \omega(t)b + J \frac{d\omega}{dt} + T_l(t) \quad (3.11)$$

Where  $T_d(t)$  = Develop torque

$\omega(t)$  = Rotor angular frequency

$b$  = Viscous friction

$J$  = Moment of inertia

$T_l(t)$  = Load torque



The electromagnetic torque produced by a BLDC motor can be expressed as:

$$\begin{aligned}
 T_d(t) &= k_{t-a}i_a + k_{t-b}i_b + k_{t-c}i_c \\
 e_a &= K_e\omega_m(t) \\
 T_e &= \frac{e_a i_a + e_b i_b + e_c i_c}{\omega_m}
 \end{aligned} \tag{3.12}$$

Substitute equation (3.4), (3.5) and (3.6) into (3.12):

$$\begin{aligned}
 T_e &= \frac{(K_e f(\theta_e) \omega_m) i_a + (K_e f(\theta_e - \frac{2\pi}{3}) \omega_m) i_b + (K_e f(\theta_e + \frac{2\pi}{3}) \omega_m) i_c}{\omega_m} \\
 T_e &= K_e \left[ f(\theta_e) i_a + f(\theta_e - \frac{2\pi}{3}) i_b + f(\theta_e + \frac{2\pi}{3}) i_c \right]
 \end{aligned} \tag{3.13}$$

Where  $T_e$  = Electromagnetic torque [Nm]

$K_e$  = Torque constant [Nm/A]

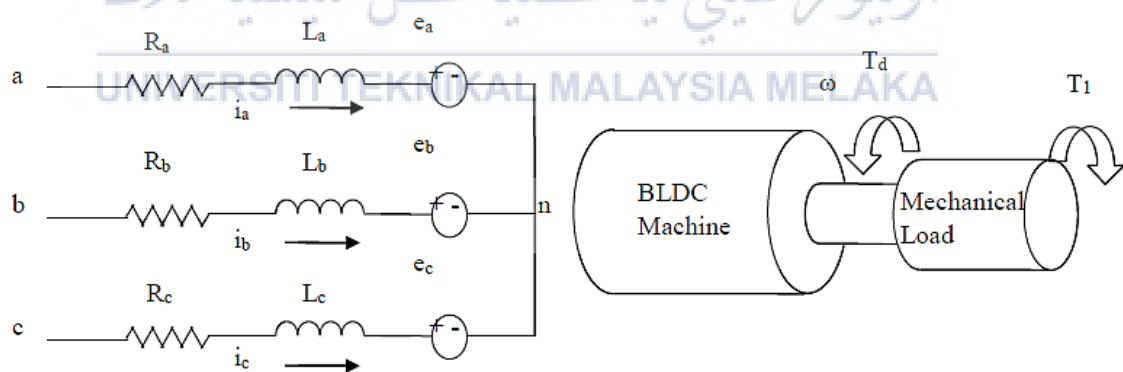
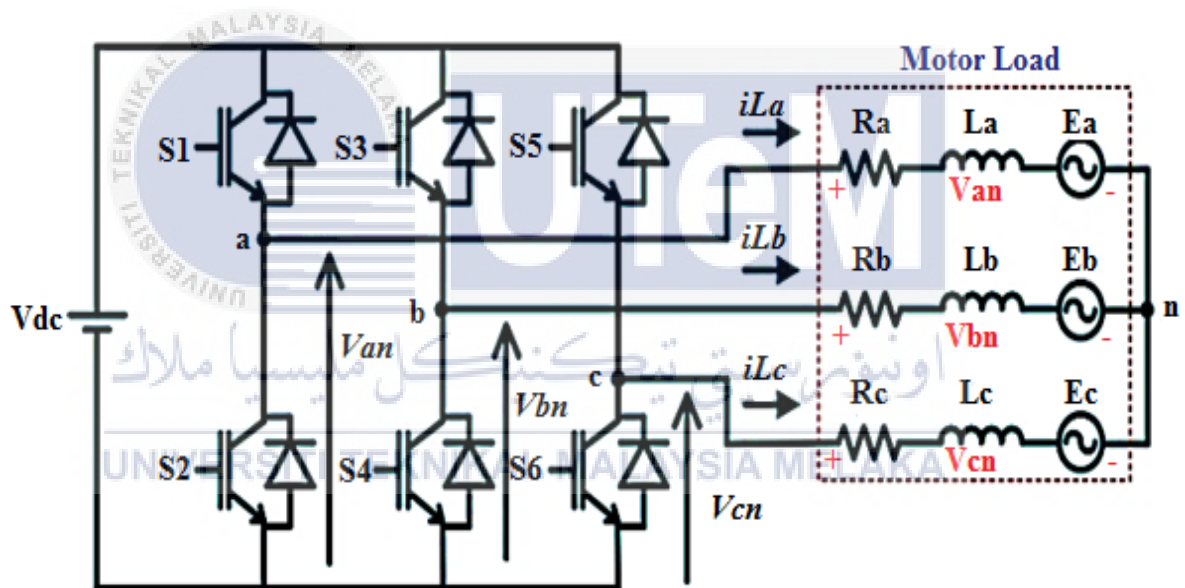


Figure 3.1: Three phase BLDC Machine Equivalent Circuit and Mechanical Model

### 3.3 Voltage Source Inverter (VSI)

Figure 3.2 shows a topology circuit and a simplified circuit of three-phase voltage source inverter (VSI). The three-phase VSI is connected to the wye-winding of an induction machine. Note that, the upper and lower switches for every phase of simplified VSI can be represented by a toggle switch since the switching of upper and lower IGBTs are complementary to each other. This means the switching state of each phase, i.e.  $S_a^+$ ,  $S_b^+$  or  $S_c^+$  equals to 1 when the upper switch of the leg is ON and the lower switch is OFF, otherwise, the switching state equals to 0.



(a)

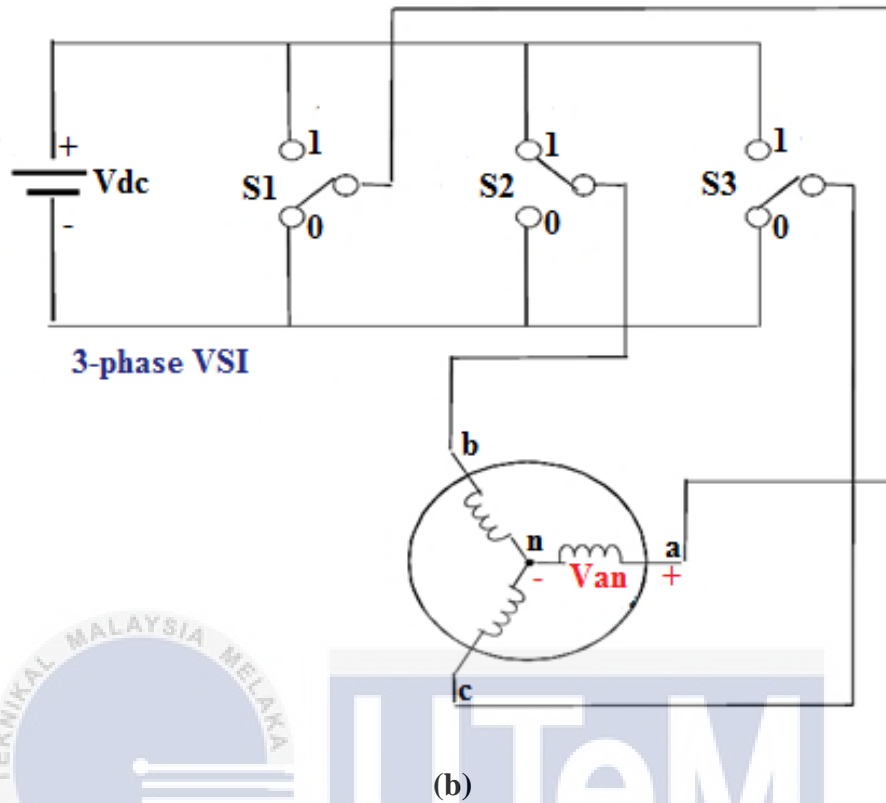


Figure 3.2: Three-Phase Voltage Source Inverter (a) Topology Circuit (b) Simplified Circuit

### 3.4 Principle Operation of Torque Hysteresis Controller

This section is about principle operation of Torque Hysteresis Controller (THC). Hysteresis Operation is explained with diagram of hysteresis current control and output graph. Besides, topology circuit of hysteresis with structure of THC for BLDC motor is also included in this section.

### 3.4.1 Hysteresis Operation

In order to operate the BLDC motor and achieve an objective and its purpose, suitable controller need to be used. Proposed strategy is important to make sure that controller selected gives better performance operation for BLDC motor. Torque Hysteresis Controller (THC) is selected method since to overcome the Voltage Controlled method to control both torque and current for BLDC motor. THC overcomes the drawback of conventional approaches which produce overshoot current since THC provides protection of current. The error in the bandwidth reduced to force variable control stay close to the reference value. THC strategy contain one current loop structure. Current and torque are proportional to each other, therefore once the current can be controlled, torque easily be control. Desired torque defined from the current reference generated by the current control creates from THC. As there is torque reference, torque demand can be achieved by it. Furthermore, THC is a simple method and gives more excellent performance on BLDC motor compared with voltage controlled.

Figure 3.3 shows block diagram of hysteresis current controller. The conventional or basic implementation of hysteresis current controller gives the output of switching signal,  $S_x$  ( $S_a$ ,  $S_b$  and  $S_c$ ) that will send to three phase inverter by comparing current error,  $I_{error}$  with a fixed hysteresis band. The actual current,  $I_{act}$  refers to the load current components such as  $I_a$ ,  $I_b$  and  $I_c$  from the output of inverter. To activate the power switches of inverter, output currents error are used [6]. The switching of inverters important as to make sure that BLDC motor runs smoothly. Switching ON or OFF in the predefined gap can be determined by hysteresis current control and it's clearly the most important things in THC method. Hysteresis current control compared the signal with the reference current in its bandwidth. There are two bands, upper and lower bands. If the actual current touches the upper band, the output signal is 1 and whereas if the actual signal touches the lower band, output signal is 0. Figure 3.4 shows the output graph of hysteresis current control.

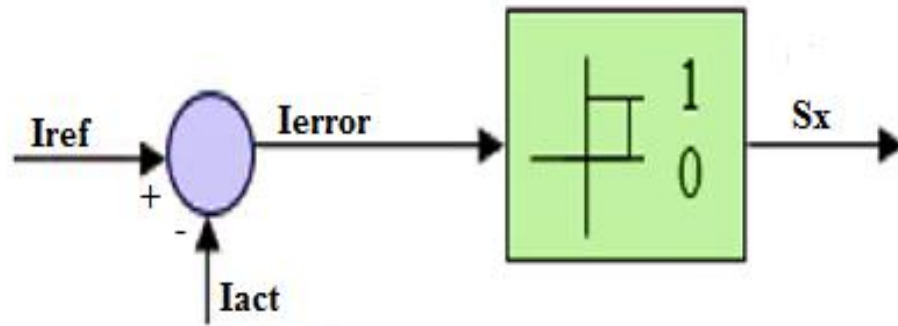


Figure 3.3: Block Diagram of Hysteresis Current Controller

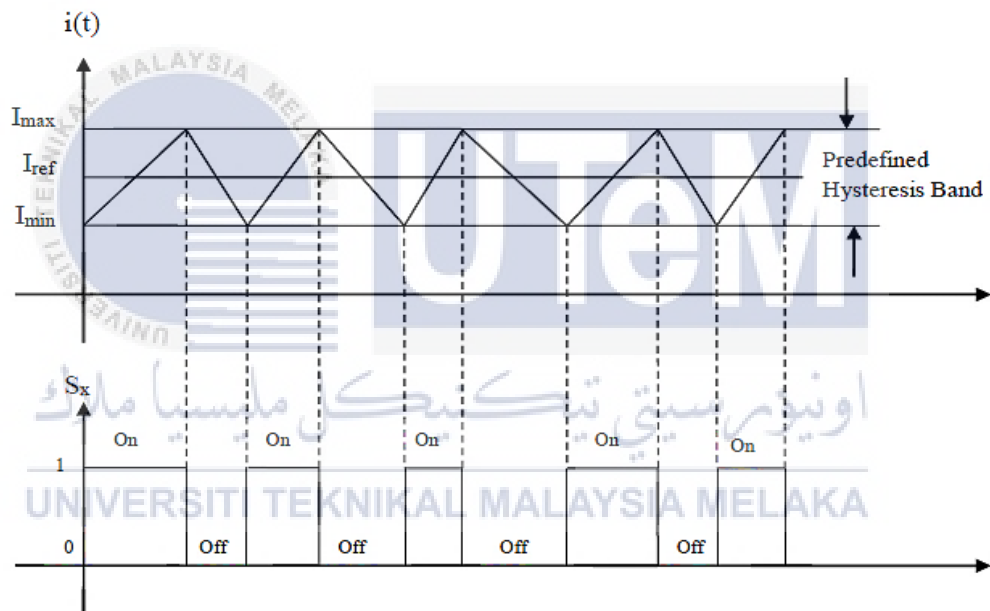


Figure 3.4: Output Graph of Hysteresis Current Switching Control

### 3.4.2 Topology Circuit

Torque Hysteresis Controller (THC) is a method chosen to replace conventional approaches which is Voltage Controlled. Since the inrush current during start-up in the voltage controlled, THC is used to overcome the disadvantages in order to control both torque and current. THC also can limit the current since it has one loop current control. Hysteresis control method is one of the simplest close loop control since it forces the variable controlled restricted within the bandwidth follow it reference value. With THC method, BLDC motor can achieve excellent torque dynamic performance. As shown in Figure 3.5, two-level hysteresis comparator is used in order to control the current phases. Besides, it can help to generate proper switching state that later supply to the inverter as to read increases and decreases value on phase current as long the error of ripple current stay within the hysteresis band.

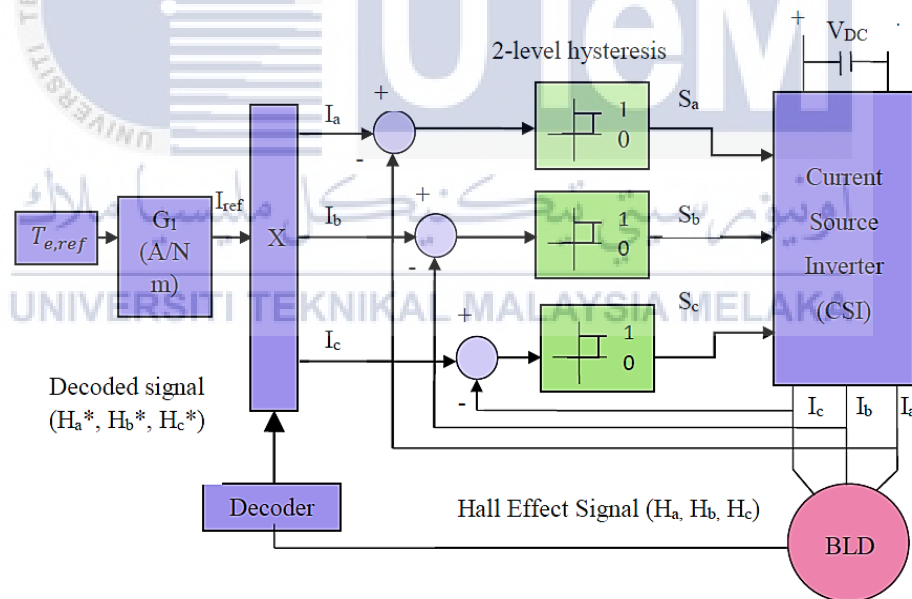


Figure 3.5: Structure of Torque Hysteresis Controller (THC) for BLDC motor

### 3.5 Simulation Model of BLDC Motor

This section is about simulation model of BLDC Motor. There are two simulation models, Conventional Implementation and Proposed Method of Torque Hysteresis Controller. All methods described on how to construct their simulation model.

#### 3.5.1 Simulation Model for Conventional Implementation of Torque Hysteresis Controller

Two-level hysteresis comparator is used in order to control the current phases. Besides, it can help to generate proper switching state that later supply to the inverter as to read either increases or decreases value on phase current as long the error of ripple current stay within the hysteresis band. Furthermore, pattern of waveform for each reference current will similar to their decoded signals as shown in Table 3.

Table 3.0: Derivation of Decoded Signals based on Hall Effect Signals

Hall Effect Signals			Decoded Signals		
H <sub>a</sub>	H <sub>b</sub>	H <sub>c</sub>	H' <sub>a</sub>	H' <sub>b</sub>	H' <sub>c</sub>
0	0	0	0	0	0
0	0	1	0	-1	+1
0	1	0	-1	+1	0
0	1	1	-1	0	+1
1	0	0	+1	-1	0
1	0	1	0	+1	-1
1	1	0	0	+1	-1
1	1	1	0	0	0

Figure 3.6 is a simulation of decoder circuit where it is build referred to the Hall Effect Sensor. Incremental Encoder is produced by it as shown in Table 3.1. The system will smoothly run as the sequence of VSI achieved with the accuracy of signal triggered Figure 3.7 shows complete Torque Hysteresis Controller (THC) simulation circuit of Brushless DC Motor by using MATLAB 2016b software. This circuit consists of two-level hysteresis, subsystem contains of three phase inverter, permanent magnet synchronous machine and decoder for Hall Sensor Effect. Besides, from this circuit, output waveform such as torque ( $T_e$ ), speed ( $\omega_m$ ) and three phase current ( $i_a$ ,  $i_b$ ,  $i_c$ ) produced. Analyzation from the output waveforms needed to compare between conventional and proposed implementation of THC.

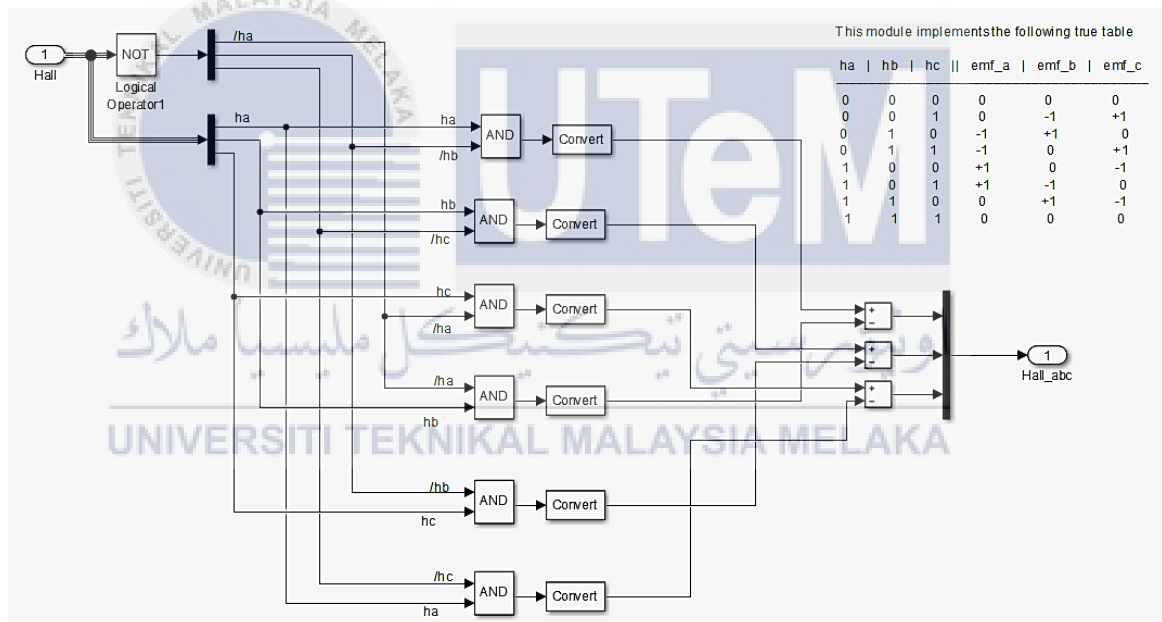


Figure 3.6: Simulation of Decoder Circuit



Table 3.1: Hall Effect Sensor and Incremental Encoder Table

HA	HB	HC	EMFA	EMFB	EMFC
0	0	0	0	0	0
0	0	1	0	-1	+1
0	1	0	-1	+1	0
0	1	1	-1	0	+1
1	0	0	+1	0	-1
1	0	1	+1	-1	0
1	1	0	0	+1	-1
1	1	1	0	0	0

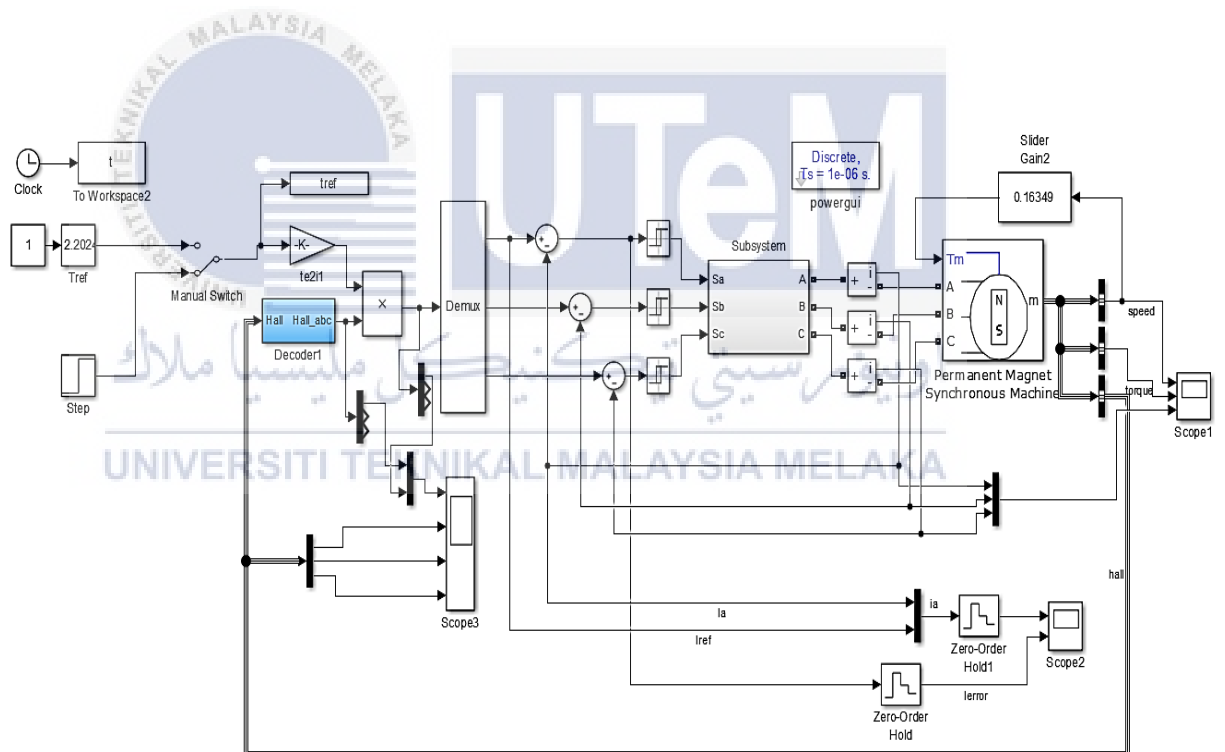


Figure 3.7: Complete Block Diagram of Simulation Control for BLDC Motor

### 3.5.2 Simulation Model for Proposed Method of Torque Hysteresis Controller

Simulation for Conventional Implementation of Torque Hysteresis Controller consists of Decoder Circuit where Hall Effect Sensor with logic (0 and 1) to be convert into Back EMF current (0, -1 and +1). In decoder circuit, it consists of differential amplifier where when convert it into analog devices the output may error or not accurate to 5V. Furthermore, conventional implementation circuit also consists of multiplier. It's possible to use all logic devices for the circuit. To avoid using differential amplifier and multiplier, new logic circuit drawn to replace the conventional implementation so analog ICs easily be used in this project.

The derivation of incremental encoder table obtained from decoder circuit used for proposed new method of THC as shown in Table 3.2. As shown in Figure 3.8, the top IGBTs are S1, S3 and S5. Positive currents for Ia, Ib and Ic needed to ON the top IGBT. As example in Figure 3.9, S1 will turn ON when Ia positive current for Hall Effect Sensors 100 and 101. It will produce Ha and Hb. By using the AND gate, the output of two halls will be controlled with the reference based on Hysteresis A. Similar to S3 and S5, selected halls for positive Ib and Ic with control by Hysteresis B and Hysteresis C. Therefore, top IGBT will be controlled based on hall and hysteresis.

Table 3.2: Hall Effect Sensor, Current and Switching State Table

HALL EFFECT SENSOR			BACK EMF CURRENT			SWITCHING STATE OF INVERTER					
Ha	Hb	Hc	Ia	Ib	Ic	S1	S2	S3	S4	S5	S6
0	0	1	0	-	+	OFF	OFF	OFF	ON	SW	OFF
0	1	0	-	+	0	OFF	ON	SW	OFF	OFF	OFF
0	1	1	-	0	+	OFF	ON	OFF	OFF	SW	OFF
1	0	0	+	0	-	SW	OFF	OFF	OFF	OFF	ON
1	0	1	+	-	0	SW	OFF	OFF	ON	OFF	OFF
1	1	0	0	+	-	OFF	OFF	SW	OFF	OFF	ON

\*SW= Switching for top IGBT

From Figure 3.8, bottom IGBTs are S2, S4 and S6. Bottom switches will always ON to give negative currents of  $I_a$ ,  $I_b$  or  $I_c$ . Figure 3.9 shows the logic circuit for bottom IGBT of S4. For S4, negative current of  $I_a$  for Hall Effect Sensor 010 and 011. From the two halls with negative current of  $I_a$  produced  $H_c$  and  $H_b$  then S4 will turn ON. The negative current will support the positive current flows from top IGBT.

Figure 3.10(a) shows the three-phase inverter with BLDC motor phases. Top IGBTs will switching ON or OFF based on Hall Effect Sensor but for bottom IGBTs will always ON to give negative current. Figure 3.10(b) shows an example of operation for Hall Effect Sensor 001. Back EMF current gives  $I_c$  positive and  $I_b$  negative. The top IGBT that switching ON is S3 while bottom IGBT that gives negative current is S5. The current will flow from phase C to phase A. Figure 3.11 shows complete circuit or block diagram of proposed method Torque Hysteresis Controller (THC) for BLDC motor. This circuit doesn't have any differential amplifier or multiplier but only consist of logic gate which better in implementation of analog ICs.

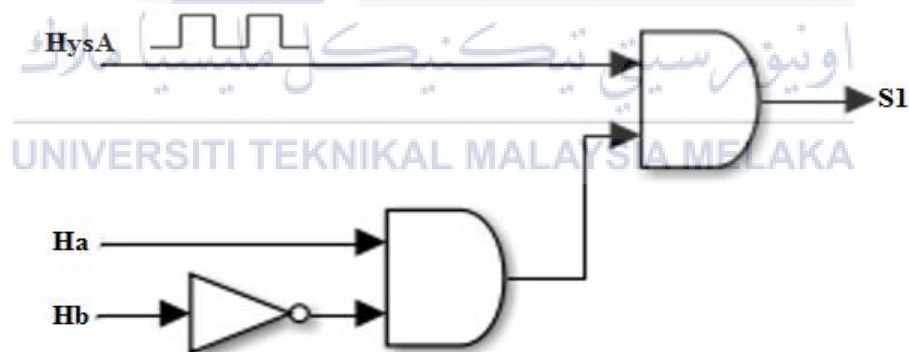


Figure 3.8: Logic Circuit for top IGBT of S1



Figure 3.9: Logic Circuit for bottom IGBT of S4

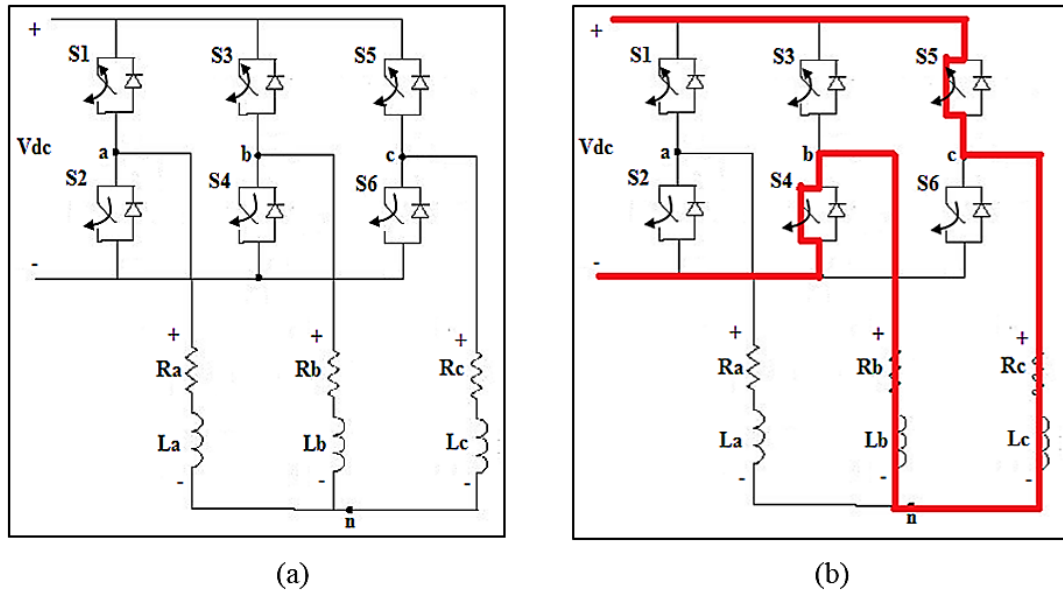


Figure 3.10: Switching of IGBT and Current Phases (a) Normal (b) Hall 001

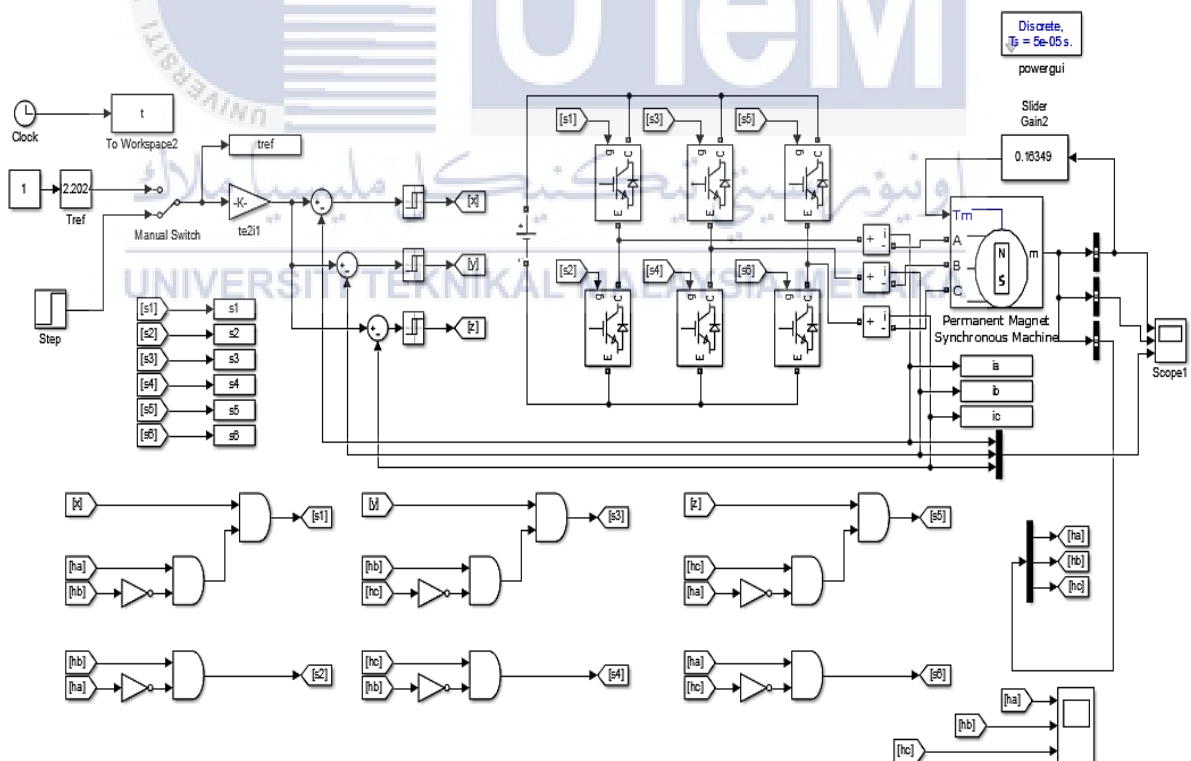


Figure 3.11: Complete Block Diagram of Proposed Method for BLDC Motor

### 3.6 Experimental Setup

This section is about detailed explanation on experimental setup for basic or conventional implementation of Torque Hysteresis Controller (THC) by using dSPACE 1104. Furthermore, proposed method experimental setup also well explained in this section with a figure of it.

#### 3.6.1 Conventional Implementation using dSPACE 1104

The conventional implementation is designed by using dSPACE 1104 R&D Controller Board along with other components such as direct current power supply system (48V), I/O terminal, BLDC Hall Sensor Terminals, Gate Driver Circuit and three-phase inverter. There are also current transducer (CT) and powder brake as a loading unit. A dSPACE is used to interconnect the software and hardware so that the driver in the motor can be controlled. The flow of experimental setup for conventional implementation as shown in figure 3.13 with sampling time of 40 $\mu$ s.

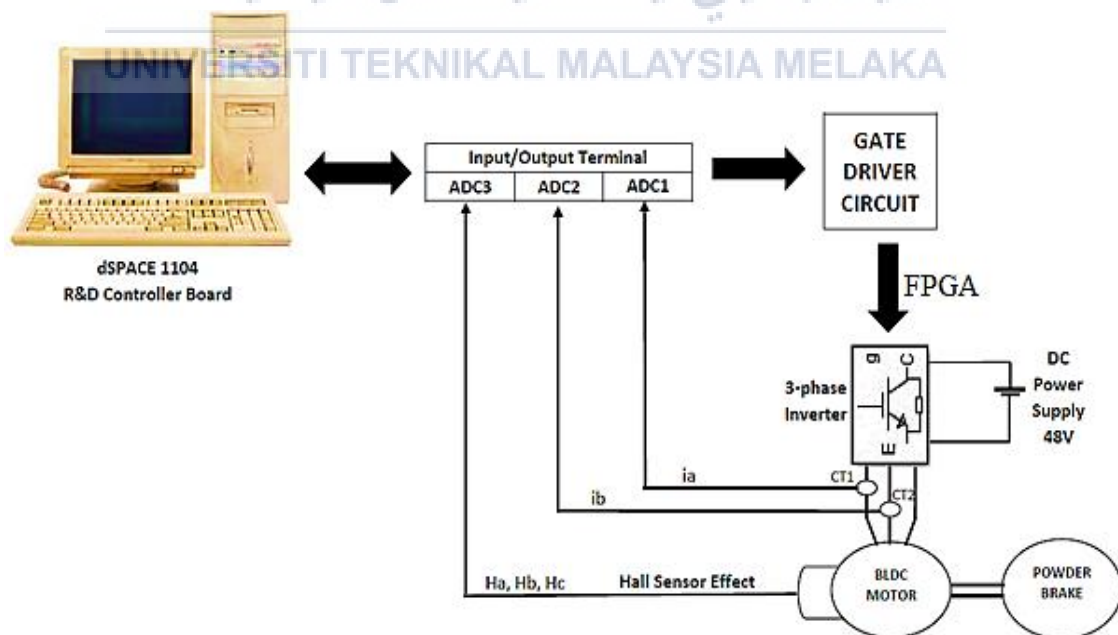


Figure 3.12: Experimental Setup for Conventional Implementation

### 3.6.2 Proposed Experimental Setup

The proposed method is fully analog ICs setup by having three phase circuit of current sensor, hysteresis current controller, hall encoder or hall sensor signal detector, logic circuit and inverter. All the circuits and gate driver with BLDC motor are controlled and supplied by function generator and display to the oscilloscope. Figure 3.13 shows the arrangement of Printed Circuit Board (PCB) or experimental setup for proposed method. Besides, detailed schematic for all designed PCB or circuit are explained. Next, the important of each integrated circuits (ICs) used in every PCB are well elaborated too.

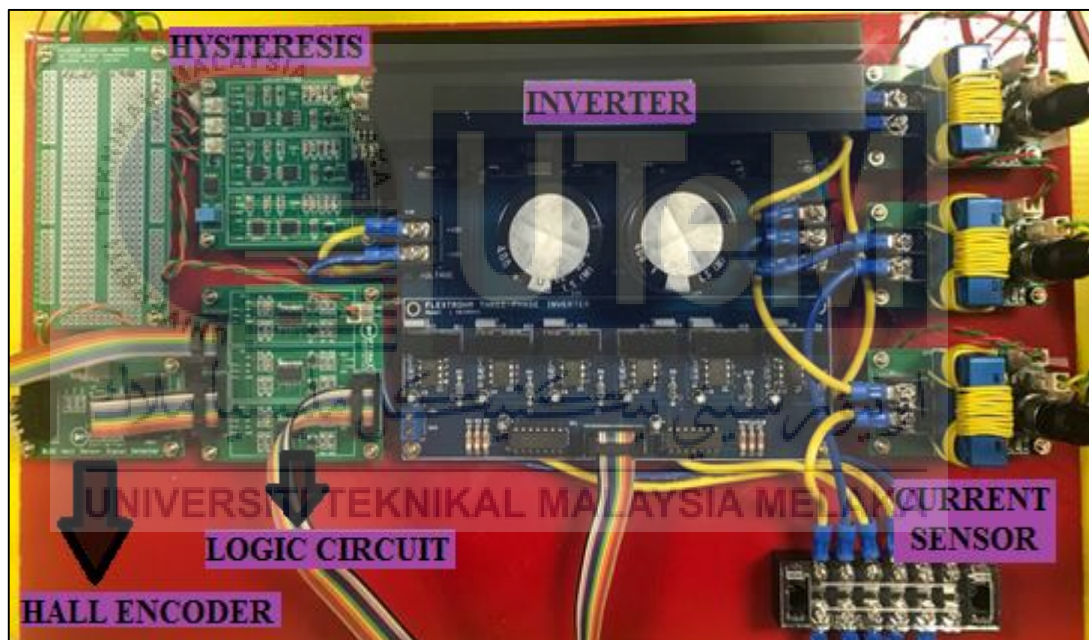


Figure 3.13: Experimental Setup for Proposed Method

### 3.6.2.1 Hall Sensor Signal Detector

Figure 3.14 and Figure 3.15 show the schematic and Printed Circuit Board for Hall Sensor Signal Detector. Hall Sensor Signal Detector is used to transfer signal from BLDC motor to the logic circuit. By using 14 legs of surface mount device (SMD) SN74LS07 as open-collector to transfer logic function (0 and 1) from BLDC motor to logic circuit. The input signals known as H1, H2 and H3 from BLDC motor. The signals will flow through the buffer and generate output signal Ha, Hb and Hc which later be used in Logic Circuit [15]. The overview data sheet of SN74LS07 as shown in Appendix D.

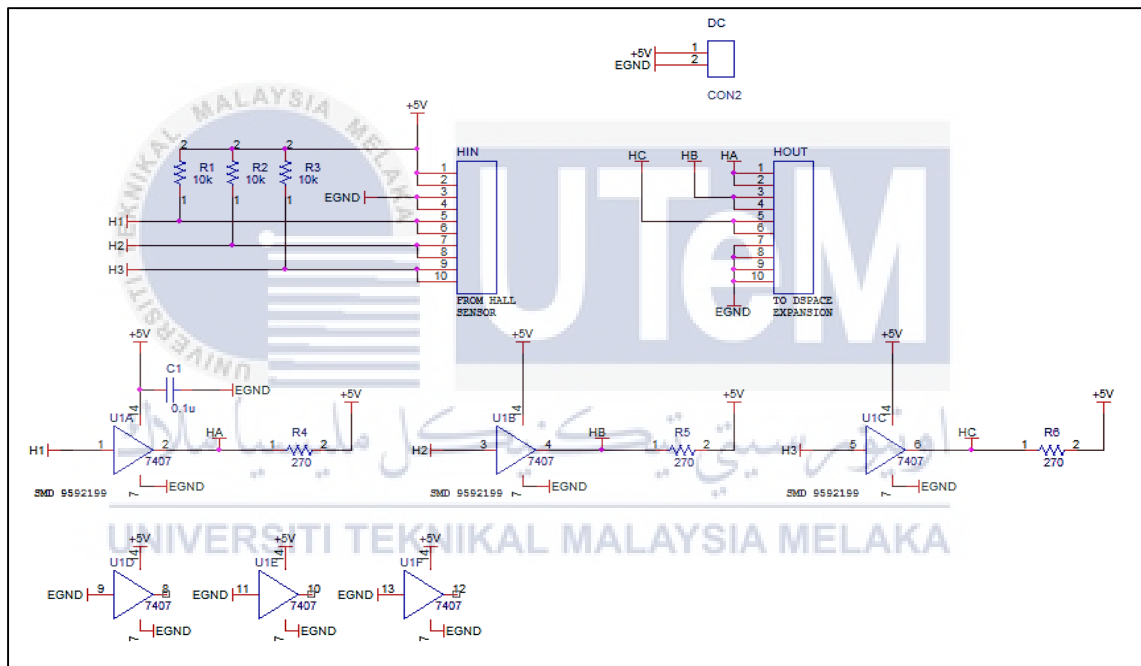


Figure 3.14: Schematic of Hall Sensor Signal Detector



Figure 3.15: PCB of Hall Sensor Signal Detector

### 3.6.2.2 Hysteresis Current Controller

As shown in Figure 3.16 and Figure 3.17, the schematic circuit drawn in Orcad 9.2 software and PCB of Hysteresis Current Controller (HCC). Hysteresis Current Controller is used to generate output current follows its reference in the limit bandwidth. There are few ICs used in this circuit such as Voltage Regulator (LM7805C), Voltage Reference (ADR381), Differential Amplifier (AD8276), Op-Amp (AD8022) and Hysteresis Comparator (TLV3201). This circuit is designed with three-phases where it is compared the current from current sensor to the reference current and obtained the error. The error will flow to the hysteresis comparator and the output of hysteresis status will send to the logic circuit.

Hysteresis comparator operates within two bands, upper band (UB) and lower band (LB). As there is an input signal and assume the initially output signal is zero. The input signal gradually increasing and the output signal remains zero. Once input signal



touch the upper band, the output signal changes to high or 1. Output signal will remain high or 1 until the input signal touched the lower band and changed it to low or zero output signal. The schematic drawn by referring to the data sheet named TLV3201 as given in the Appendix G. The AD8022 is a voltage-feedback op amp designed especially for applications requiring very low voltage and current noise along with low supply current, low distortion, and ease of use. These dual amplifiers provide wideband, with high output current optimized for stability when driving capacitive loads. This low noise op amp can be operating at wide supply range which are  $\pm 5\text{V}$ ,  $\pm 2.5\text{V}$  to  $\pm 12\text{V}$  power supply. Data sheet of AD8022 as given in Appendix C.

The AD8276 is purposely, unity-gain difference amplifiers intended for precision signal conditioning in power critical applications that require both high performance and low power. AD8276 consists of a low power and low noise op amp. Advantages of the integrated resistors of the AD8276 provides the designer with several benefits over a discrete design, including smaller size, lower cost, and better ac and dc performance. Data sheet of AD8276 is given in Appendix F. The ADR381 is 2.500 V band gap voltage references featuring high accuracy, high stability, and low power consumption in a tiny footprint. The wide operating range and low power consumption make them ideal for 3V to 5V battery-powered applications. From the schematic, the input is 5V and the output is 2.5V. The data sheet of ADR381 as given in Appendix E.

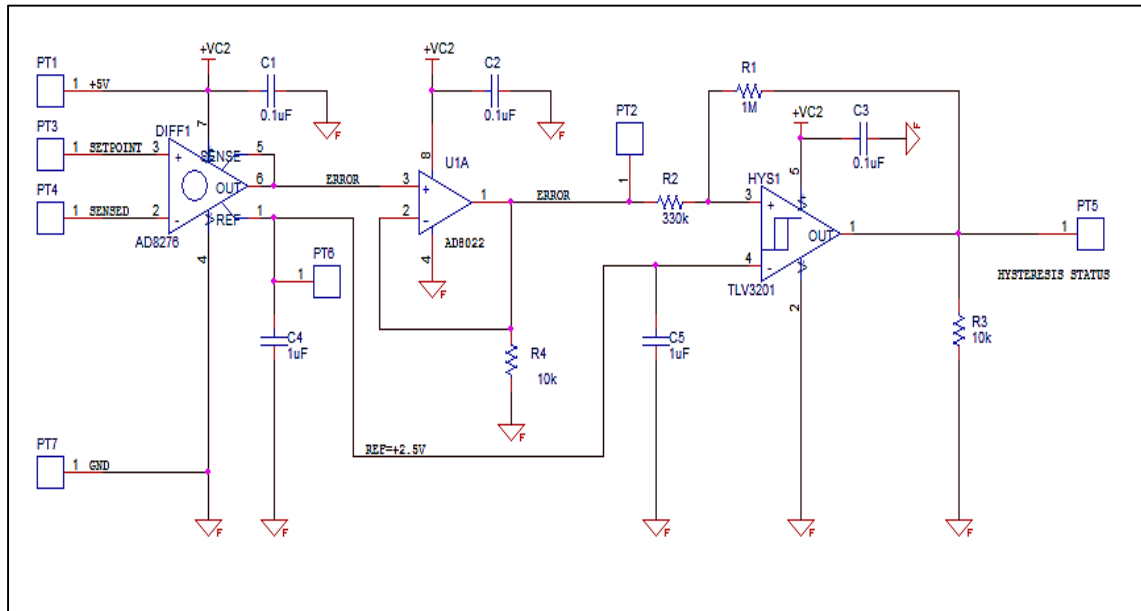


Figure 3.16: Schematic of Hysteresis Current Controller

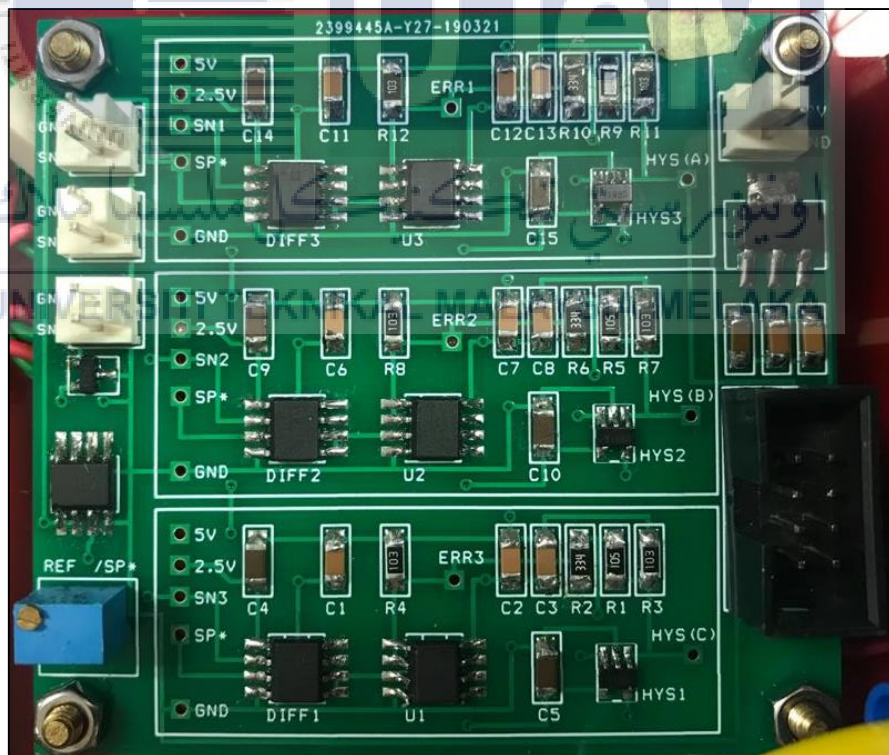


Figure 3.17: PCB of Hysteresis Current Controller

### 3.6.2.3 Logic Circuit

Figure 3.18 and Figure 3.19 show the schematic and PCB of Logic Circuit. In this Logic Circuit, NOT and AND gate is used. By using this two gates, hysteresis status from Hysteresis Current Controller and hall signal from Hall Sensor Signal Detector are combined to form a switching status (S1 to S6). There are 3 layers of Logic Circuit for different switching status which are S1 and S2, S3 and S4 and last but not least S5 and S6. All the switching status will be used for three-phase inverter. Switching status S1, S3 and S5 are used to turn ON the top IGBTs where S2, S4 and S6 for the bottom IGBTs.

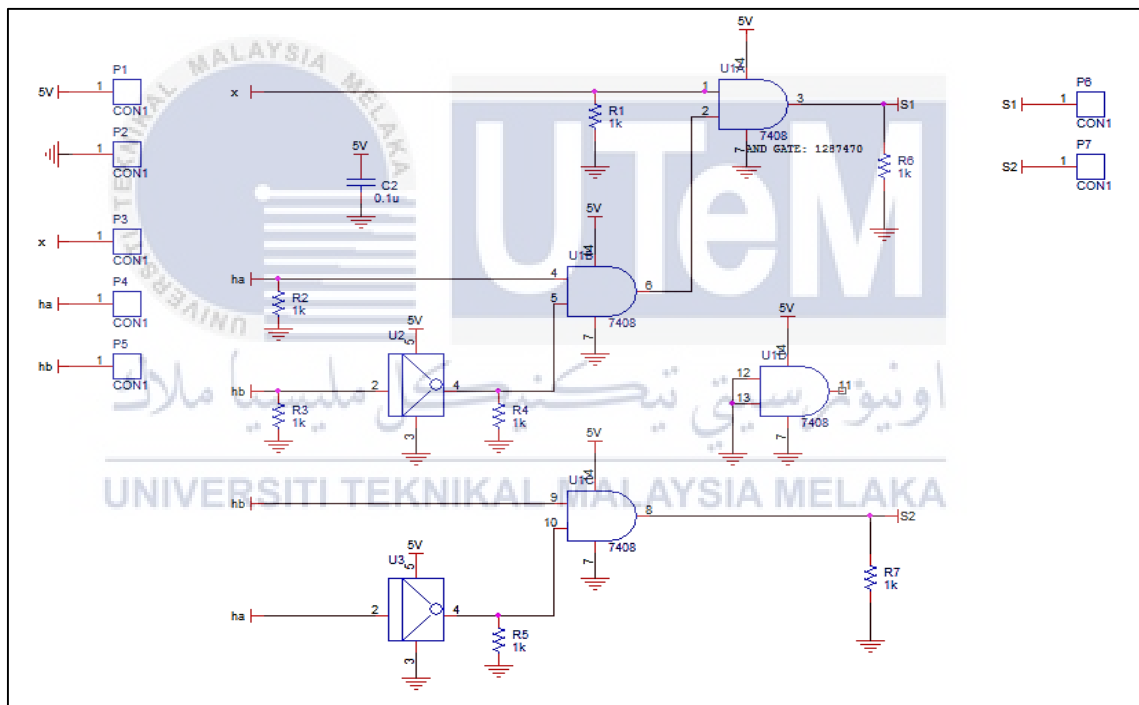


Figure 3.18: Schematic of Logic Circuit

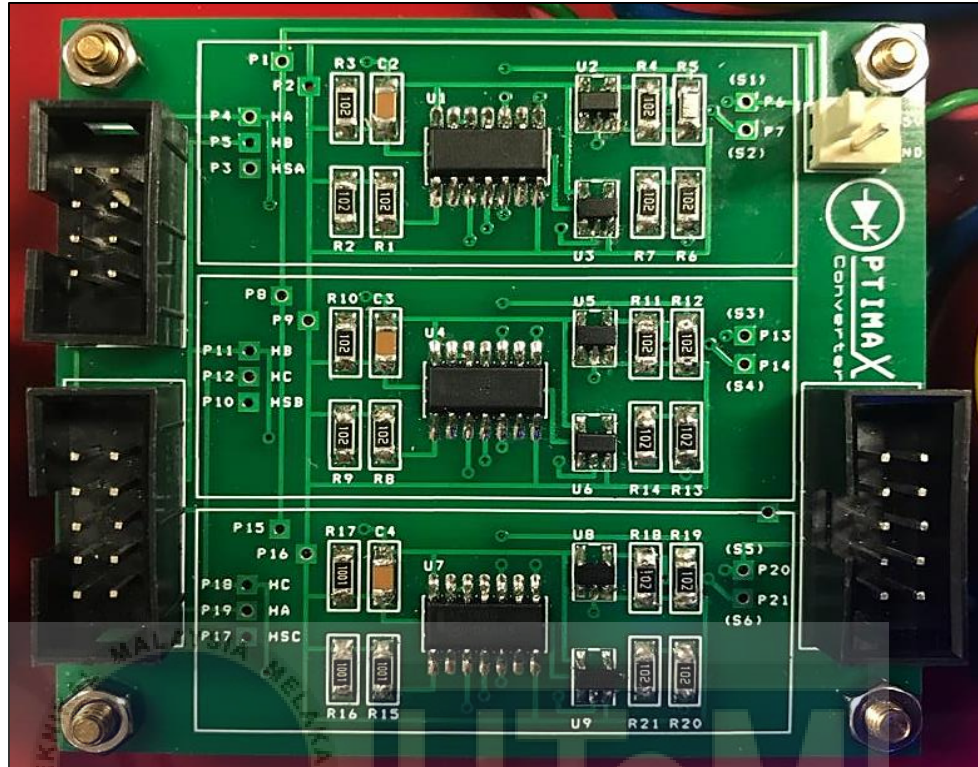


Figure 3.19: PCB of Logic Circuit

#### 3.6.2.4 Current Sensor

Figure 3.20 and Figure 3.21 show the schematic and PCB of current sensor. This circuit is using blue current sensor type of LEM Open Loop Current Sensor. There are 20 windings of wire that have been done manually. This current sensor will detect current in a wire and generate signal proportional of current. Besides, in this circuit, it's also consists of Voltage Regulator (LM7805C), Voltage Reference (ADR381) and an Op-Amp (AD8022). Voltage Regulator will regulate voltage output of 5.0V whereas Voltage Reference will regulate Voltage to reference of 2.5V.

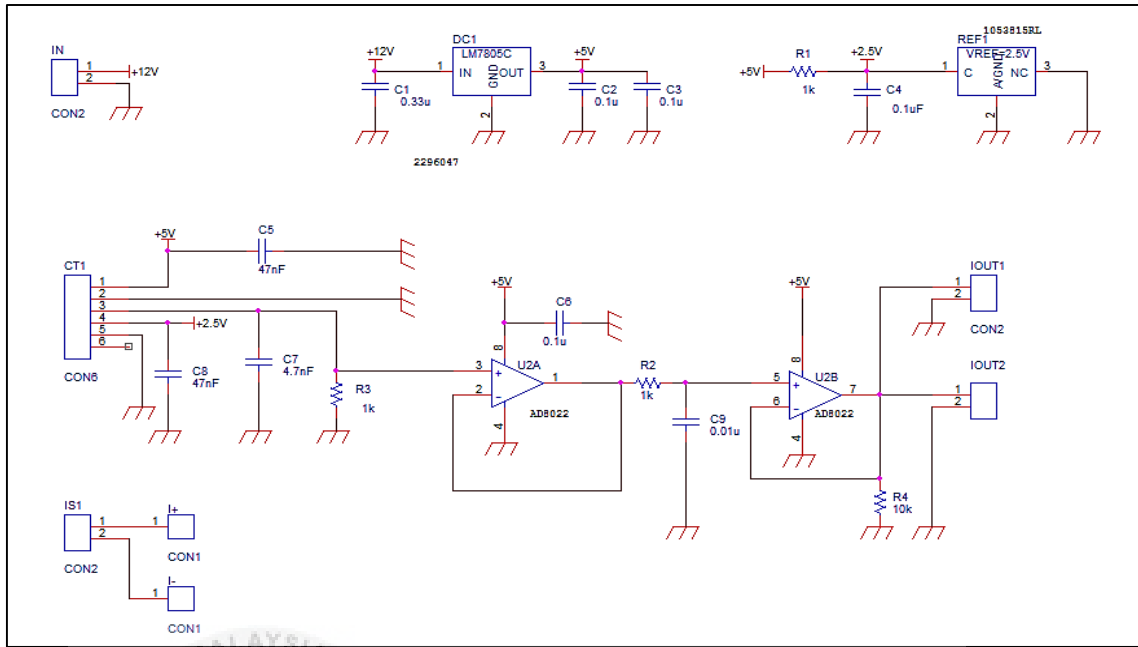


Figure 3.20: Schematic of Current Sensor



Figure 3.21: PCB of Current Sensor

## CHAPTER 4

### RESULTS AND DISCUSSION

#### 4.1 Introduction

This project is expected to achieve the desired objective which is the implementation of Torque Hysteresis Controller (THC) for BLDC motor by using proposed method. The simulation was performed by using the Simulink in MATLAB software. The results obtained from the simulation of THC for BLDC motor is analyze in terms of the current and torque produced and compared with the preliminary results, which is the Voltage Controlled of BLDC motor. Furthermore, the experimental setup results for Conventional and Proposed Method for THC also compared and described. The theory from the previous chapter will be proved in this chapter by simulation and hardware.

#### 4.2 Parameters Setting for Simulation of Proposed THC Technique for BLDC

The simulation of proposed THC method of a BLDC motor drive is undertaken using MATLAB/Simulink with a parameters setting as shown in Table 4.1. The three-phase inverter also modeled with sampling time,  $50\mu\text{s}$ . The experimental setup consists of hysteresis current control, accurate speed and position information and an appropriately size BLDC machine and load.

Table 4.1: Parameters Value for THC of BLDC Motor

TYPE OF PARAMETERS	PARAMETERS	VALUE
Control System	Hysteresis band	0.5A
	Sampling time - Digital	50 $\mu$ s
	- Analogue	1 $\mu$ s
BLDC Motor	Stator phase resistance $R_s$ ( $\Omega$ )	0.18 $\Omega$
	Stator phase inductance $L_s$ (H)	8.5mH
	Flux linkage established by magnets	0.07145 V.s
	Back EMF flat area	120°
	Voltage Constant ( $V_{peak}$ L-L / krpm)	59.8578
	Torque constant	0.5716 Nm/A
	Moment of inertia, J	0.00062 kg.m <sup>2</sup>
	Viscous damping, F	0.0003035 N.m.s
	Static Friction, $T_f$	0 N.m
	Trap	0.5
	Pole pairs, P	4

### 4.3 Simulation Results

In this section, it is about the simulation results on Conventional Implementation and Proposed Method of Torque Hysteresis Controller (THC). The simulation results with the graph output is given. The results are also well described in this section.

#### 4.3.1 Conventional Implementation of THC

Figure 4.3 shows the schematic circuit for conventional implementation of THC. The circuit is set with sampling time of 50 $\mu$ s to show that the delay happened in

conventional implementation. The circuit consists of two-level hysteresis, subsystem represents three-phase inverters and block of permanent magnet synchronous machine in Matlab/Simulink library which produced outputs of speed, torque and Hall Effect signal. The circuit is similar to the structure of Torque Hysteresis Controller (THC). As shown in Figure 4.4, the simulation results of conventional implementation with sampling time of  $50\mu\text{s}$ . In the figure, hysteresis band sets up to  $0.5\text{A}$ , the ripple of torque and current are larger. Since the delayed in sampling time of  $50\mu\text{s}$ , the current tend overshoot out from the bandwidth. That's the main problems which later want to overcome by using THC with proposed method.

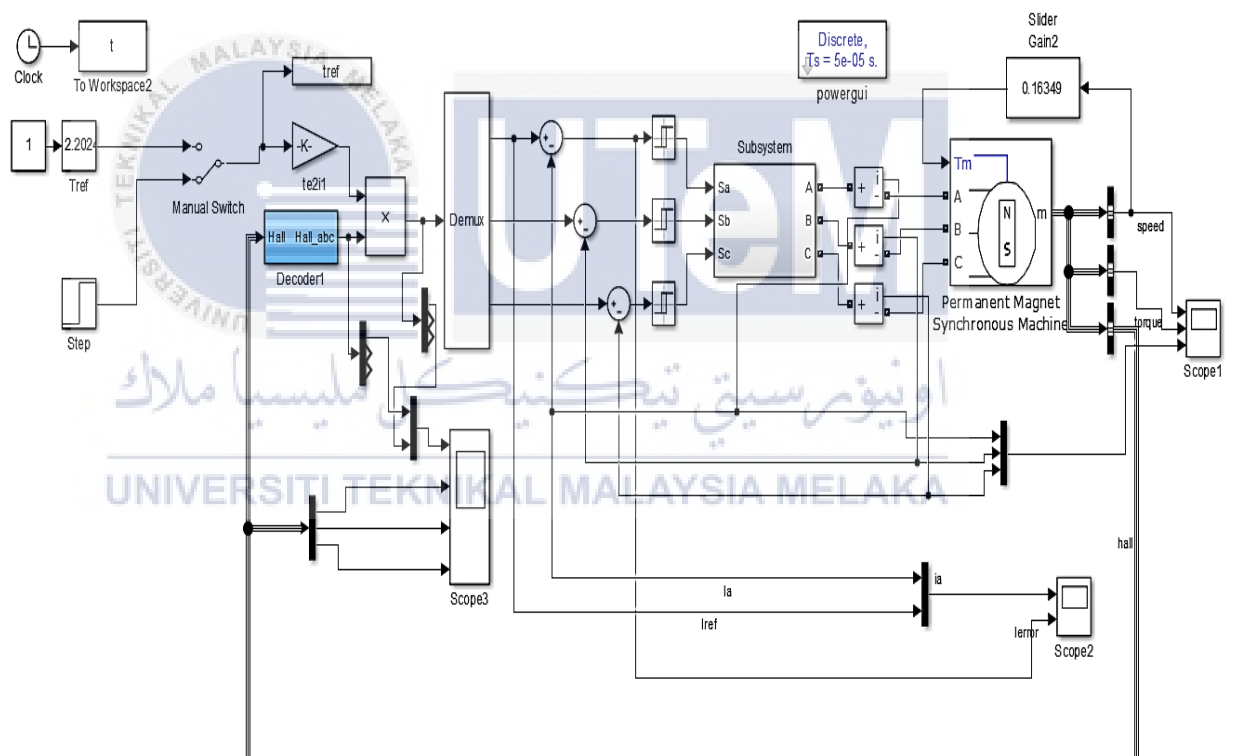


Figure 4.1: Schematic Circuit for Conventional Implementation



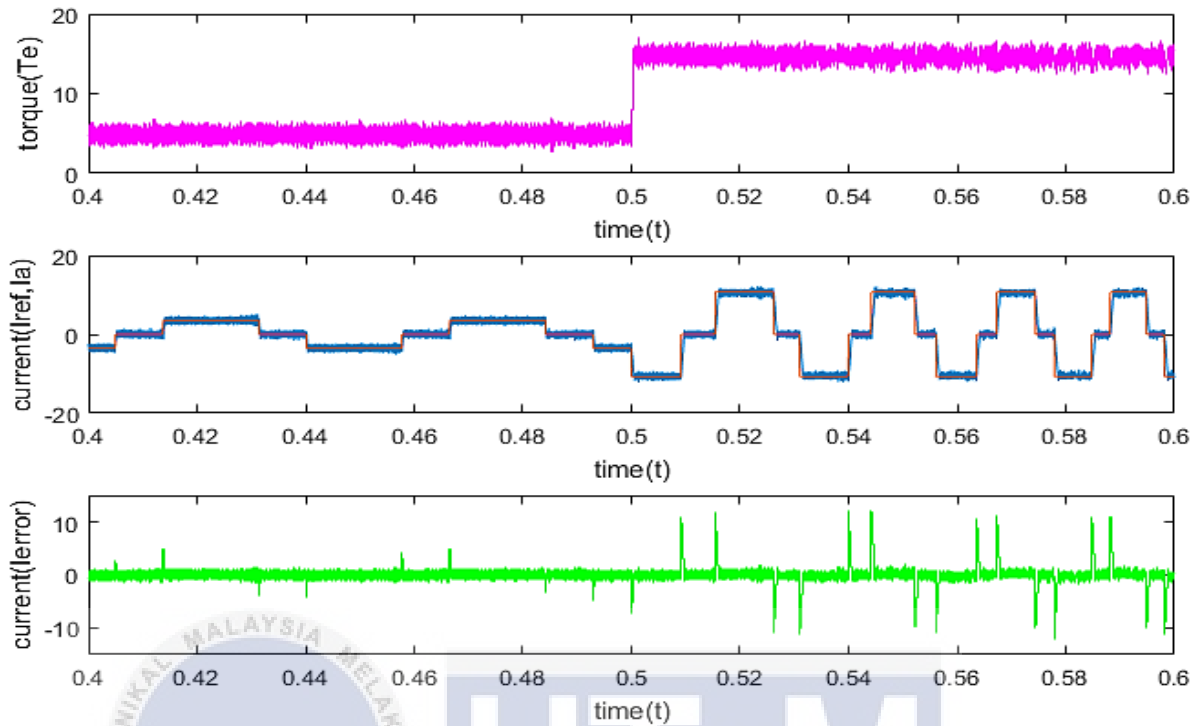


Figure 4.2: Simulation results for Conventional Implementation

#### 4.3.2 Proposed Method of THC

Figure 4.3 shows the simulation designed for a proposed method by using fully analogue ICs to implement it for BLDC motor. This new method replaced the conventional implementation where hall decoder was removed since it has three back EMF signal (positive, negative and zero current). The new proposed method represents by the logic circuit so as well as it can be used analogue ICs. Figure 4.4 shows the output waveform of current, speed and torque for proposed method with fully using analogue ICs. During the zero reference of current, there is no switching happen. There are only positive and negative switching. This two conduction mode operation gives a result on improvement of efficiency to this method due to low switching frequency. But there is an advantage with this method. During the transition positive to zero or zero to positive of

current, there is an inrush torque happen. This is due to delay transition to the current. The delay may effect to the performance of torque.

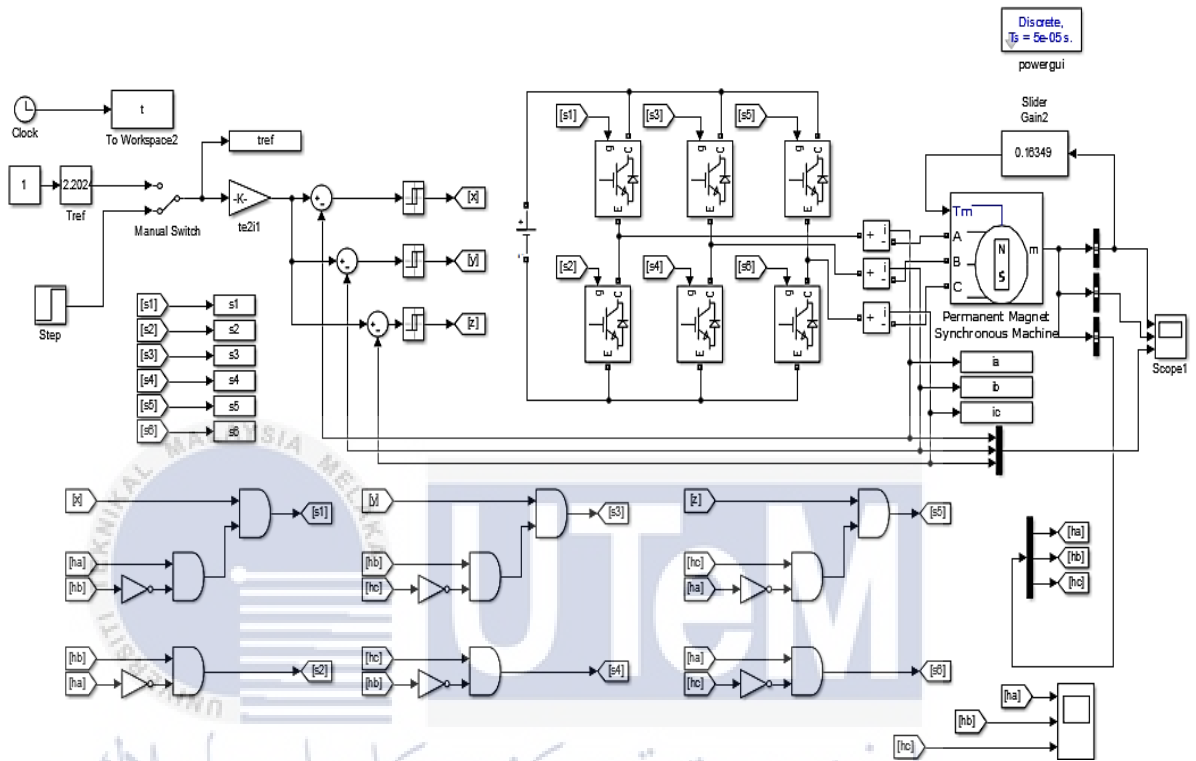


Figure 4.3: Schematic Circuit for Proposed Method

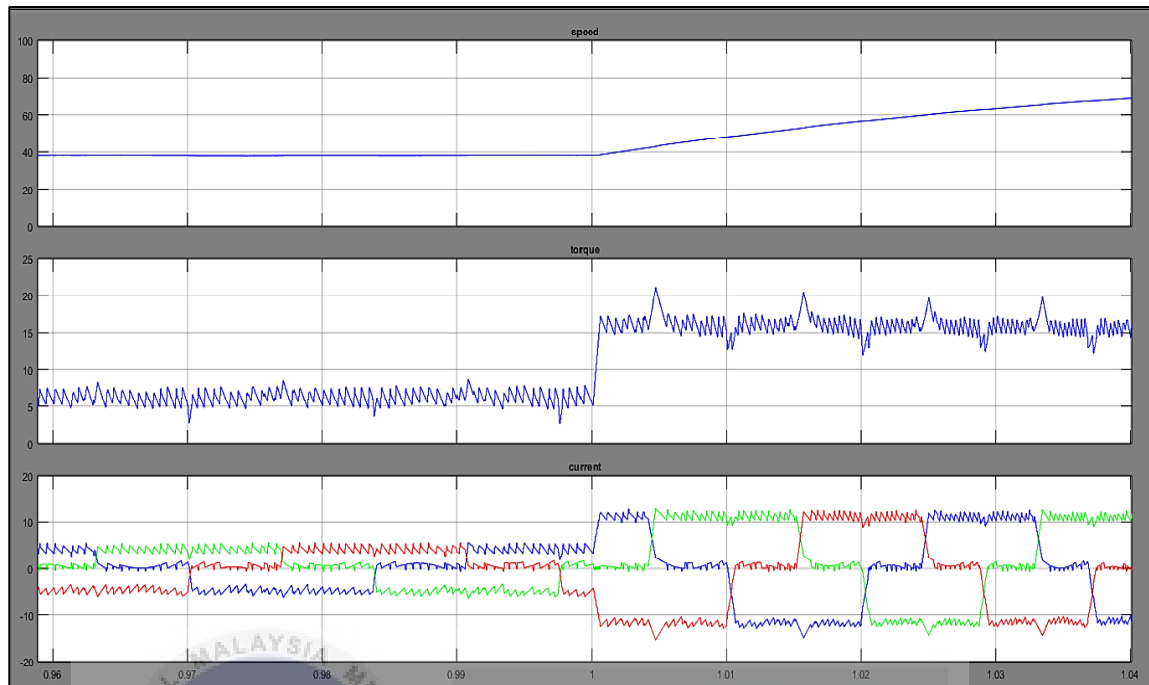


Figure 4.4: Simulation results for Proposed Method

## 4.4 Experimental Results

In this section, it is about the experimental results on Conventional and Proposed Implementation of Torque Hysteresis Controller (THC). The results from the oscilloscope with output graph is given. The results are also well described in this section.

### 4.4.1 Conventional Implementation using dSPACE 1104

Conventional Implementation of Torque Hysteresis Controller (THC) is using relation between Hall Sensor Effect with decoded signal for each phases. Figure 4.5, 4.6 and 4.7 represent the experimental results obtained for conventional implementation of THC with different limit of bandwidth for hysteresis. The blue, red and green graphs show the current signal for phase A, B and C. Figure 4.5 shows the result for hysteresis band of

0.0025A. All the current signals follow its' reference in square-sin wave. Switching happen at positive, negative and zero current. In this conventional implementation, the current can't be controlled in the restricted band. The current tend to overshoot out of the bandwidth. The hysteresis band for Figure 4.6 is 0.1A while Figure 4.7 is 0.5A. The larger the bandwidth of hysteresis, the larger the ripple of current signals. As the larger the band of hysteresis such as 0.5A, the shape of waveform for current signal can't be seen smoothly. That's the problem that will overcome through the proposed method soon.

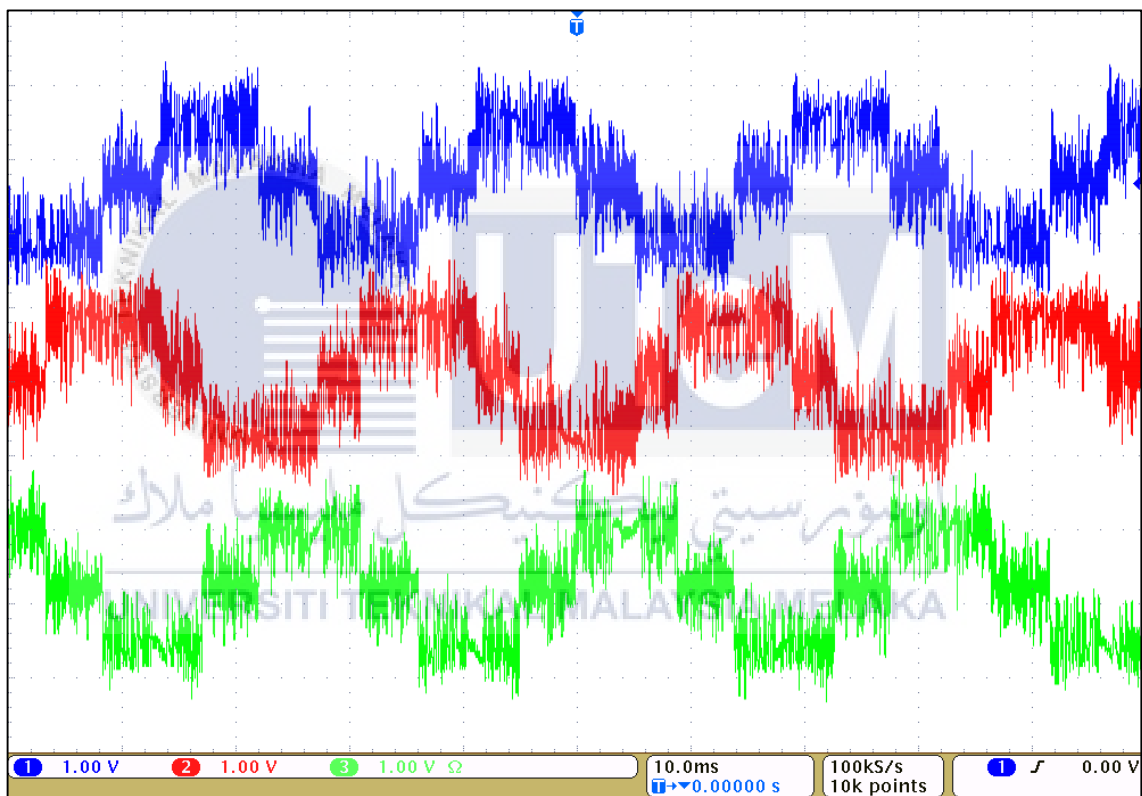


Figure 4.5: Results for Bandwidth 0.025A

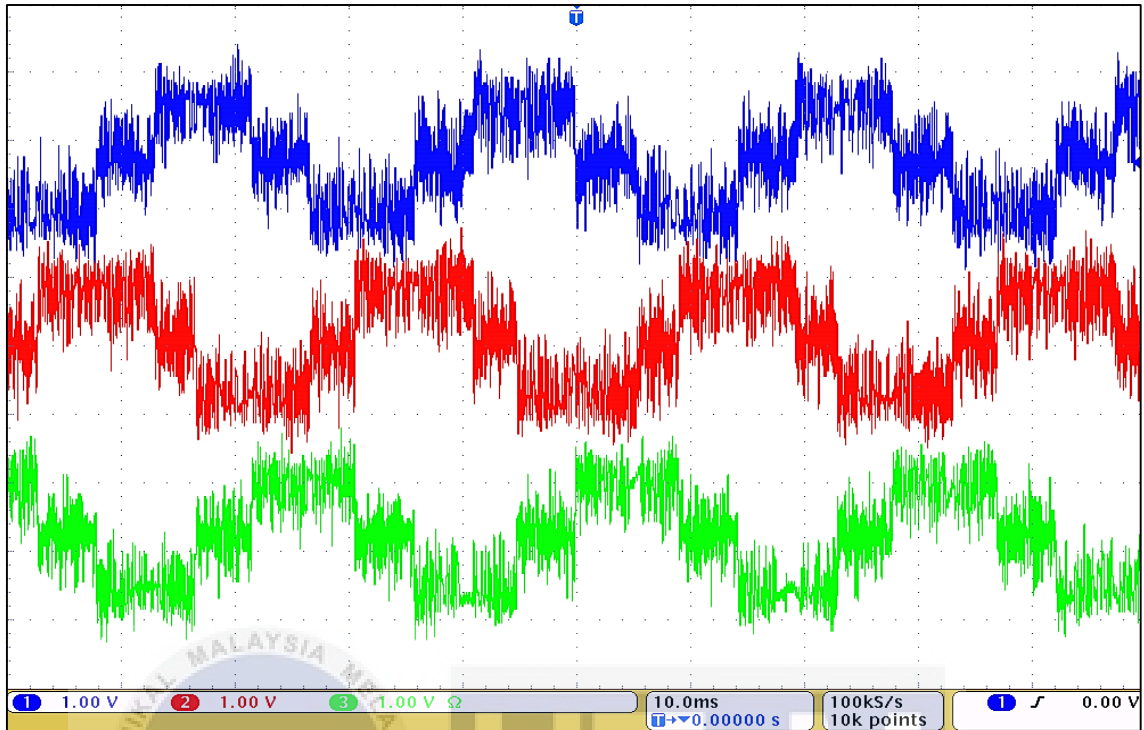


Figure 4.6: Results for Bandwidth 0.1A

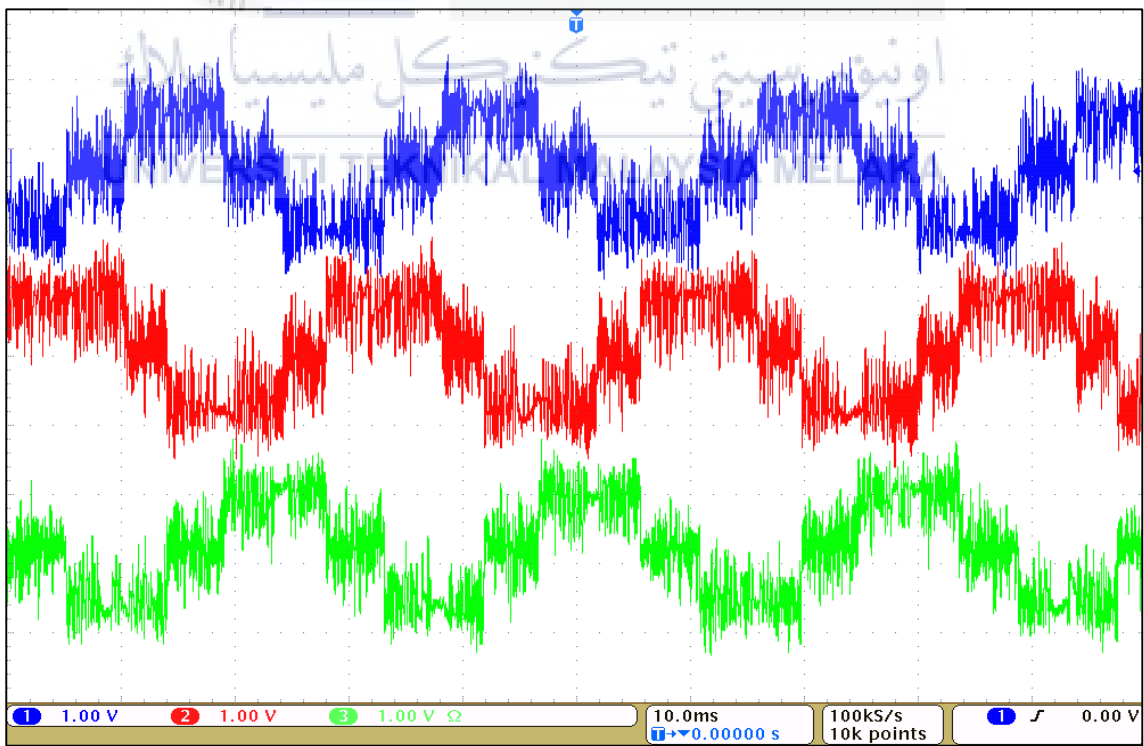


Figure 4.7: Results for Bandwidth 0.5A

#### 4.4.2 Proposed Method of THC

The proposed method of Torque Hysteresis Controller (THC) experimental setup is by using fully analog implementation. Due to some problems, hysteresis current controller and logic circuit part can't make it when they were combined with inverter, current sensor and hall sensor detector. There is problem with the hysteresis PCB due to limitation of reference can't achieve to 2.5V. The output from voltage reference should be 2.5V but after tested it's only 1.0V. Due to insufficient supply to three-phase hysteresis circuit, the single IC of voltage reference can't make the output of 2.5V as reference value.

Even though the experimental setup was unsuccessful, the hysteresis current controller and logic circuit will be represented by using dSPACE 1104 as shown in Appendix B. Figure 4.8 shows the bandwidth for hysteresis of 0.025A while Figure 4.9 for 0.1A and last but not least Figure 5.0 for 0.5A. The blue, red and green waveform represents the current signal for phase A, B and C respectively. As shown in the results, at the zero current signal, there is no switching happens. The switching of current occurs during the positive and negative sequence. As for it, this method can improve the efficiency in current control due to low switching frequency. It shows that low losses happen in this implementation. Next, this method provides two conduction mode of operation since there is no switching happens in zero reference. From all the results, the higher the hysteresis band, the higher the amplitude for current waveform. Even though high bandwidth injected to this method, the waveform from current signal stay within the reference.

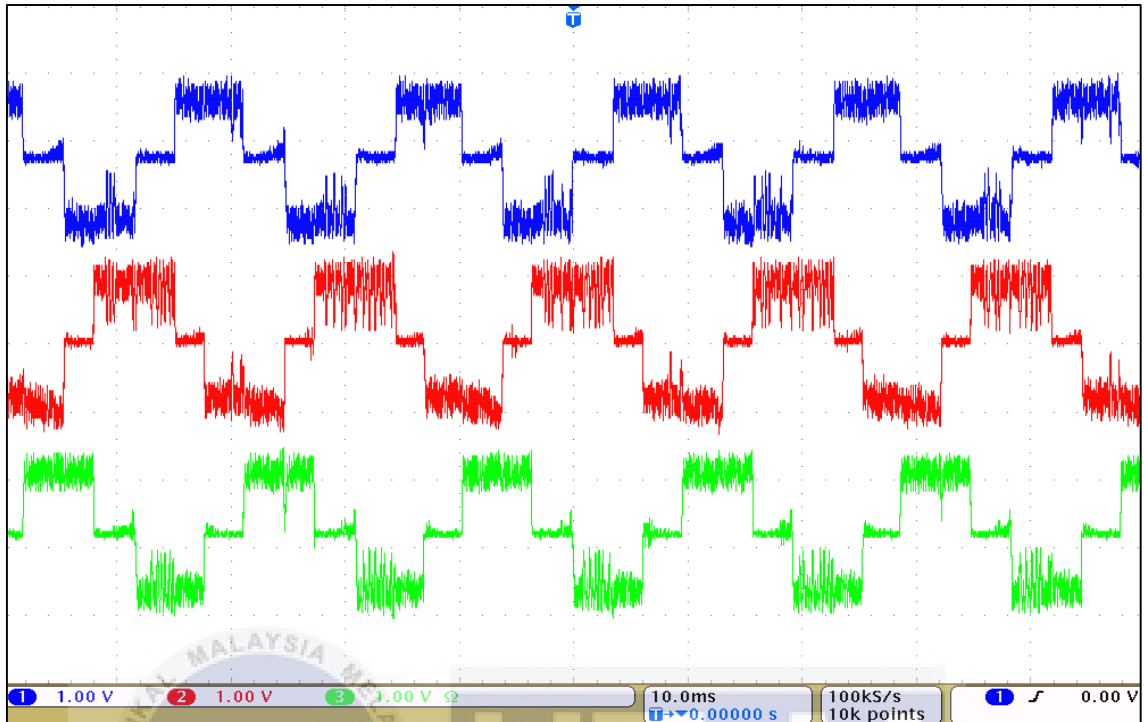


Figure 4.8: Results for Bandwidth 0.025A

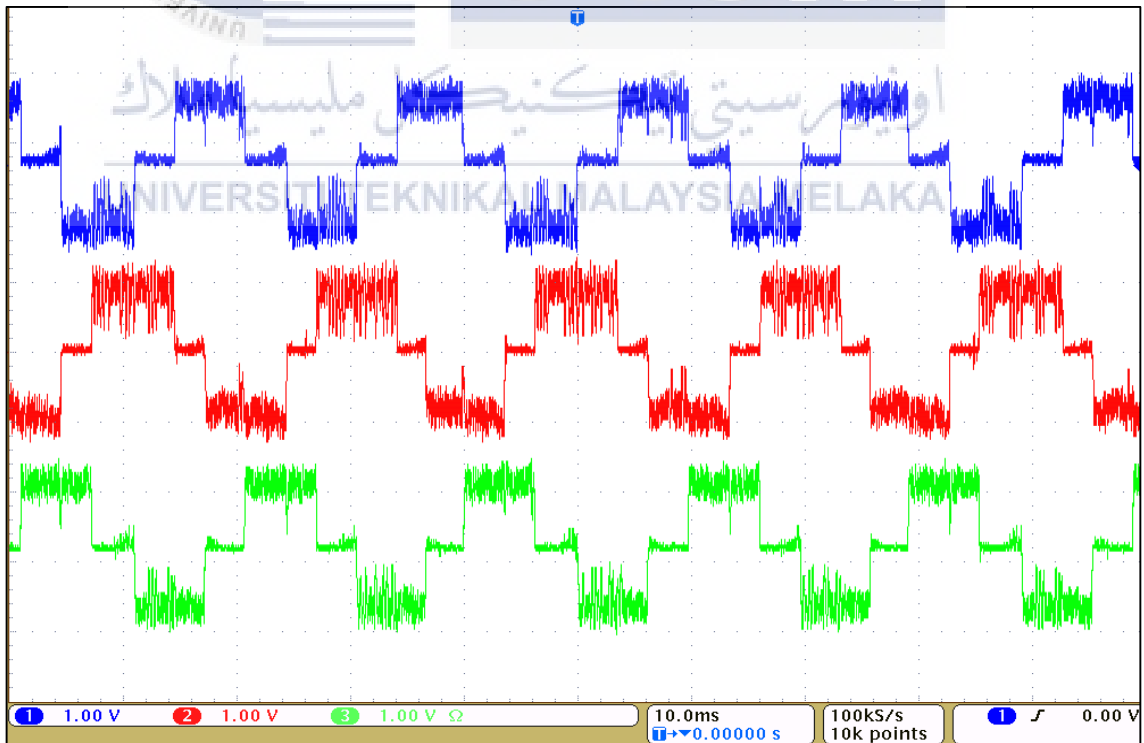


Figure 4.9: Results for Bandwidth 0.1A

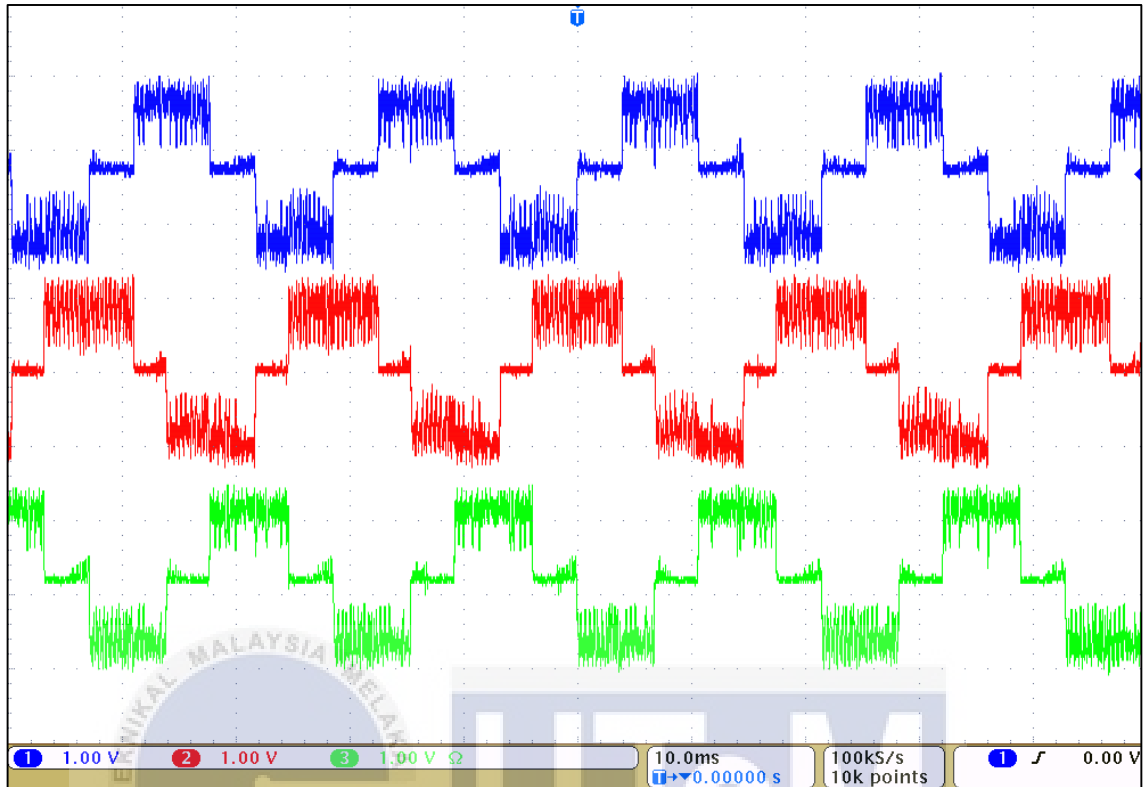


Figure 4.10: Results for Bandwidth 0.5A



## CHAPTER 5

### CONCLUSION

#### 5.1 Conclusion

In the nutshell, the whole report is mainly about the implementation of Torque Hysteresis Controller method for Brushless DC motor (BLDC). The proposed method, THC by using analogue ICs is explained by using simulation through Matlab/Simulink even though can't make it successfully in experimental setup. The other way, it is still can be prove the better performance and efficiency by using the proposed method with partially analogue PCB and dSPACE 1104. It is also proven that through THC method, the dynamic response for BLDC motor much improve than using the basic method of Voltage Controlled.

#### 5.2 Future Work

Implementation of THC by using Analogue ICs need to further studies as to shows the new method implemented through experimental setup. As to improve the waveform of new method where the torque waveform has some outshoot when the current transition from positive to negative or negative to negative due to delay transition of current.

## REFERENCES

- [1] Ismail. K.A., Kasim. R., Jidin. A., Bahari. N. Implementation of Torque Hysteresis Controller (THC) of Brushless DC Machines. IEEE Transaction, 2012.
- [2] Inc., M.T. (2007). Sensorless BLDC Control with Back-Emf Filtering.2-3.
- [3] E. S Hamidi, "Design of Small Electrical Machines". 1994.
- [4] T. Wildi, "Electrical Machines, Drives, And Power Systems Fifth Edition". 2002.
- [5] Inc., M.T. (2002). Brushless DC Motor Control Made Easy.2.
- [6] Fernando Rodriguez. Advanced Digital Control Techniques for Brushless DC Motor Drives, Dec 2006.
- [7] Zhong, L., Rahman, M. F., Hu, W. Y. & Lim, K. W. 1997. Analysis of Direct Torque Control in Permanent Magnet Synchronous Motor Drives. Power Electronics, Ieee Transactions On, 12, 528-536.
- [8] Jidin, A., Idris, N. R. N., Yatim, A. H. M., Jidin, A. Z. & Sutikno, T. Torque Ripple Minimization in Dtc Induction Motor Drive Using Constant frequency torque controller. Electrical Machines and Systems (ICEMS), 2010 International Conference on, 10-13 Oct. 2010 2010. 919-924.
- [9] Jian Zhao/Yangwei Yu. Brushless DC Motor Fundamentals Application Note. 2001
- [10] Nidec Corporation. What Is a Brushless DC Motor? 1995-2014
- [11] S.Rambabu. Master of Technology InPower Control and Drives. Department of Electrical Engineering National Institute of Technology Rourkela. 2007
- [12] Chapter 2. Brushless Dc Motor. Anna University, Chennai. 600 025
- [13] Pushek Madaan. Brushless DC Motors Part I: Construction and Operating Principles. Cypress Semiconductor. 2013

- [14] Chan, C.C., 1996. A novel wide speed range permanent magnet brushless DC motor drive for electric vehicles. *International Journal of Electronics*, 80(2), pp.235–248
- [15] Hong-Xing Wu, Shu-Kang Cheng & Cui Shu-mei, 2005. A controller of brushless DC motor for electric vehicle. *IEEE Transactions on Magnetics*, 41(1), pp.509–513.



## APPENDICES

### APPENDIX A

#### A1 GANTT CHART

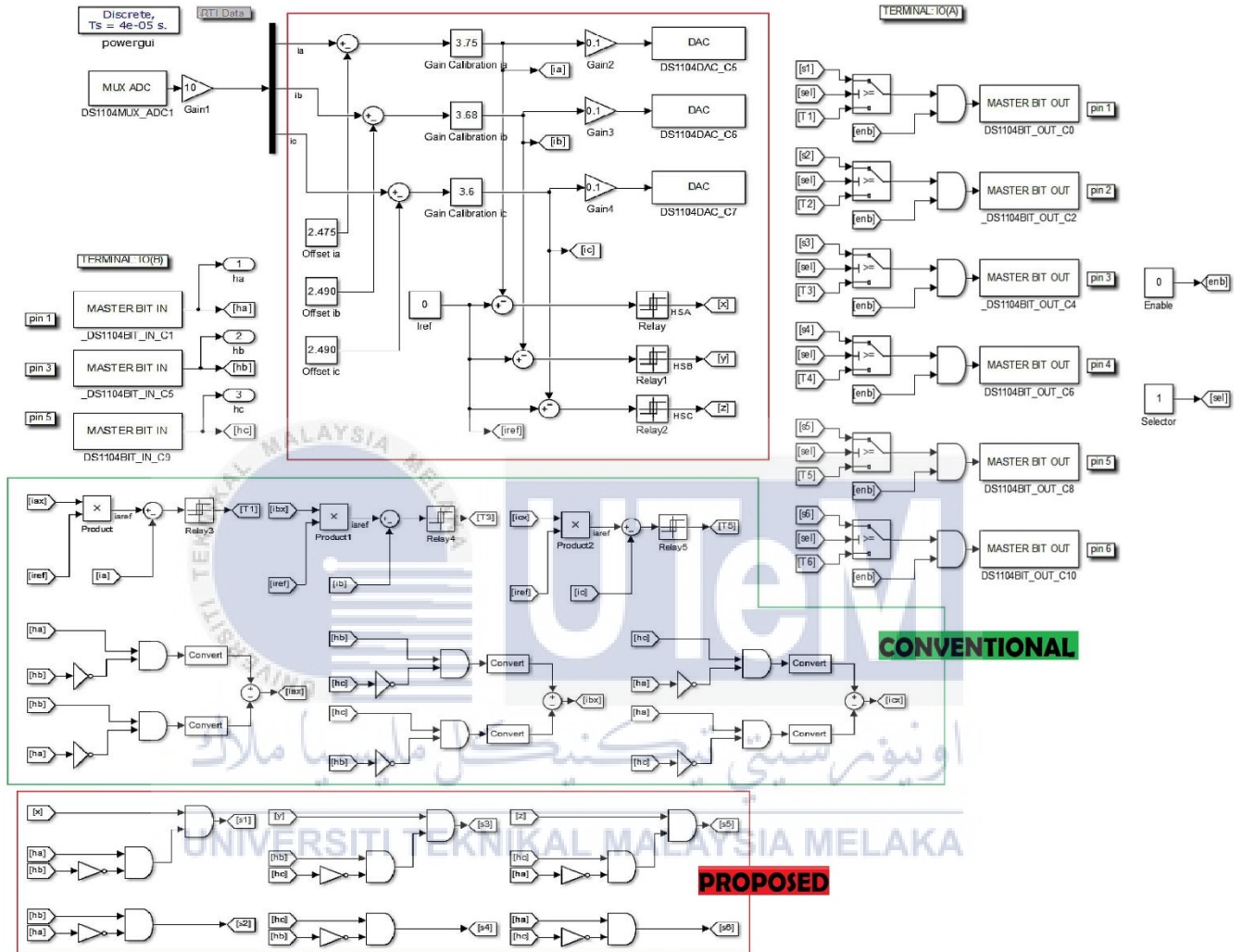
NO	FYP YEAR	FYP 1 2018														FYP 2 2019													
		WEEK														WEEK													
		1	2	3	4	5	6	7	8	9	10	11	12	13	14	1	2	3	4	5	6	7	8	9	10	11	12	13	14
1	Study on mathematical model of BLDC motor	█	█	█																									
2	Study on principle operation of THC, hysteresis operation and torque estimation				█	█	█	█	█																				
3	Study on various control technique of BLDC motor	█	█	█	█	█	█	█	█	█	█	█	█	█	█	█	█	█	█	█	█	█	█	█	█	█	█		
4	Perform simulation model and develop using Matlab software																												
5	Preparation of report and slide																												
6	Hardware implementation																												

#### A2 MILESTONES

- |    |   |                       |
|----|---|-----------------------|
| 1. | Study on mathematical model of BLDC motor                                       | 03/09/2018-30/09/2018 |
| 2. | Study on principle operation of THC, hysteresis operation and torque estimation | 01/10/2019-04/11/2018 |
| 3. | Study on various control technique of BLDC motor                                | 03/09/2018-21/04/2019 |
| 4. | Perform simulation model and develop using Matlab software                      | 05/11/2019-16/12/2018 |
| 5. | Preparation of report and slide   | 03/09/2018-19/05/2019 |
| 6. | Hardware implementation   | 18/02/2019-19/05/2019 |

## APPENDIX B

### MATLAB SIMULATION FOR DSPACE 1104



## APPENDIX C

Dual High Speed,  
Low Noise Op Amp

Data Sheet

AD8022

## FEATURES

Low power amplifiers provide low noise and low distortion,  
Ideal for xDSL modem receiver

Wide supply range: +5 V,  $\pm 2.5$  V to  $\pm 12$  V voltage supply

Low power consumption: 4.0 mA/Amp

Voltage feedback

Ease of Use

Lower total noise (Insignificant input current noise  
contribution compared to current feedback amps)

Low noise and distortion

2.5 nV/ $\sqrt{\text{Hz}}$  voltage noise @ 100 kHz

1.2 pA/ $\sqrt{\text{Hz}}$  current noise

MTPR  $< -66$  dBc (G = +7)

SFDR 110 dB @ 200 kHz

High speed

130 MHz bandwidth ( $-3$  dB), G = +1

Settling time to 0.1%, 68 ns

50 V/ $\mu\text{s}$  slew rate

High output swing:  $\pm 10.1$  V on  $\pm 12$  V supply

Low offset voltage, 1.5 mV typical

## APPLICATIONS

Receiver for ADSL, VDSL, HDSL, and proprietary  
xDSL systems

Low noise instrumentation front end

Ultrasound preamps

Active filters

16-bit ADC buffers

## GENERAL DESCRIPTIONS

The AD8022 consists of two low noise, high speed, voltage feedback amplifiers. Each amplifier consumes only 4.0 mA of quiescent current, yet has only 2.5 nV/ $\sqrt{\text{Hz}}$  of voltage noise. These dual amplifiers provide wideband, low distortion performance, with high output current optimized for stability when driving capacitive loads. Manufactured on ADI's high voltage generation of XFCB bipolar process, the AD8022 operates on a wide range of supply voltages. The AD8022 is available in both an 8-lead MSOP and an 8-lead SOIC. Fast over voltage recovery and wide bandwidth make the AD8022 ideal as the receive channel front end to an ADSL, VDSL, or proprietary xDSL transceiver design.

In an xDSL line interface circuit, the AD8022's op amps can be configured as the differential receiver from the line transformer or as independent active filters.

## FUNCTIONAL BLOCK DIAGRAM

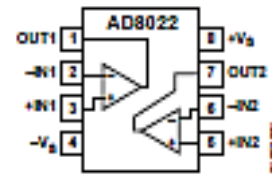


Figure 1.



UNIVERSITI TEKNIKAL MALAYSIA MELAKA

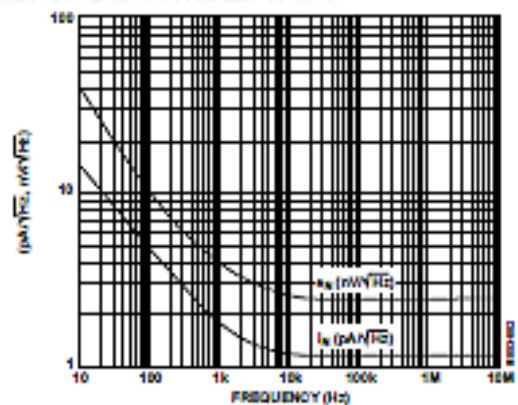


Figure 2. Current and Voltage Noise vs. Frequency

Rev. C

Information furnished by Analog Devices is believed to be accurate and reliable. However, no responsibility is assumed by Analog Devices for its use, nor for any infringements of patents or other rights of third parties that may result therefrom. Specifications subject to change without notice. No license is granted by implication or otherwise under any patent or patent rights of Analog Devices. Trademarks and registered trademarks are the property of their respective owners.

One Technology Way, P.O. Box 9106, Norwood, MA 02062-9106, U.S.A.

Tel: 781.329.4700

www.analog.com

Fax: 781.461.2112

©2011 Analog Devices, Inc. All rights reserved.

## APPENDIX D



SN74LS07

SDLS0021D –MAY 1990–REVISED APRIL 2016

## SN74LS07 Hex Buffers and Drivers With Open-Collector High-Voltage Outputs

### 1 Features

- Convert TTL Voltage Levels to MOS Levels
- High Sink-Current Capability
- Input Clamping Diodes Simplify System Design
- Open-Collector Driver for Indicator Lamps and Relays

### 2 Applications

- AV Receivers
- Audio Docks: Portable
- Blu-ray Players and Home Theaters
- MP3 Players or Recorders
- Personal Digital Assistants (PDA)
- Power: Telecom/Server AC/DC Supply: Single Controller: Analog and Digital
- Solid-State Drives (SSD): Client and Enterprise
- TVs: LCD, Digital, and High-Definition (HDTV)
- Tablets: Enterprise
- Video Analytics: Server
- Wireless Headsets, Keyboards, and Mice

### 3 Description

These hex buffers and drivers feature high-voltage open-collector outputs to interface with high-level circuits or for driving high-current loads. They are also characterized for use as buffers for driving TTL inputs. The SN74LS07 devices have a rated output voltage of 30 V. The maximum sink current is 40 mA.

These circuits are compatible with most TTL families. Inputs are diode-clamped to minimize transmission-line effects, which simplifies design. Typical power dissipation is 140 mW, and average propagation delay time is 12 ns.

#### Device Information<sup>(1)</sup>

PART NUMBER	PACKAGE (PINS)	BODY SIZE (NOM)
SN74LS07D	SOIC (14)	8.65 mm × 3.90 mm
SN74LS07DB	SSOP (14)	6.20 mm × 5.30 mm
SN74LS07N	PDIP (14)	10.30 mm × 6.35 mm
SN74LS07NS	SO (14)	10.30 mm × 5.30 mm

(1) For all available packages, see the orderable addendum at the end of the data sheet.

#### Logic Diagram (Positive Logic)



Copyright © 2016 Texas Instruments Incorporated

## APPENDIX E



## Precision Low Drift 2.048 V/2.500 V SOT-23 Voltage Reference

### ADR380/ADR381

#### FEATURES

Initial accuracy:  $\pm 5$  mV/ $\pm 6$  mV maximum  
 Initial accuracy error:  $\pm 0.24\%$ / $\pm 0.24\%$   
 Low  $TCV_{out}$ : 25 ppm/ $^{\circ}$ C maximum  
 Load regulation: 70 ppm/mA  
 Line regulation: 25 ppm/V  
 Wide operating ranges  
   2.4 V to 18 V for ADR380  
   2.8 V to 18 V for ADR381  
 Low power: 120  $\mu$ A maximum  
 High output current: 5 mA  
 Wide temperature range:  $-40^{\circ}$ C to  $+85^{\circ}$ C  
 Tiny 3-lead SOT-23 package with standard pinout

#### APPLICATIONS

Battery-powered instrumentation  
 Portable medical instruments  
 Data acquisition systems  
 Industrial process control systems  
 Hard disk drives  
 Automotive

#### GENERAL DESCRIPTION

The ADR380 and ADR381 are precision 2.048 V and 2.500 V band gap voltage references featuring high accuracy, high stability, and low power consumption in a tiny footprint.

Patented temperature drift curvature correction techniques minimize nonlinearity of the voltage change with temperature.

The wide operating range and low power consumption make them ideal for 3 V to 5 V battery-powered applications.

The ADR380 and ADR381 are micropower, low dropout voltage (LDV) devices that provide a stable output voltage from supplies as low as 300 mV above the output voltage. They are specified over the industrial ( $-40^{\circ}$ C to  $+85^{\circ}$ C) temperature range. The ADR380/ADR381 are available in the tiny 3-lead SOT-23 package.

#### PIN CONFIGURATION



Figure 1. 3-Lead SOT-23  
(RT Suffix)



Table 1. ADR38x Products

Part Number	Nominal Output Voltage (V)
ADR380	2.048
ADR381	2.500

Rev. C  
 Information furnished by Analog Devices is believed to be accurate and reliable. However, no responsibility is assumed by Analog Devices for its use, nor for any infringements of patents or other rights of third parties that may result from its use. Specifications subject to change without notice. No license is granted by implication or otherwise under any patent or patent rights of Analog Devices. Trademarks and registered trademarks are the property of their respective owners.

One Technology Way, P.O. Box 9106, Norwood, MA 02062-9106, U.S.A.  
 Tel: 781.329.4700 [www.analog.com](http://www.analog.com)  
 Fax: 781.461.2112 ©2001–2010 Analog Devices, Inc. All rights reserved.



## APPENDIX F



# Low Power, Wide Supply Range, Low Cost Unity-Gain Difference Amplifiers

Data Sheet

AD8276/AD8277

## FEATURES

- Wide input range beyond supplies
- Rugged input overvoltage protection
- Low supply current: 200  $\mu$ A maximum per channel
- Low power dissipation: 0.5 mW at  $V_S = 2.5$  V
- Bandwidth: 550 kHz
- CMRR: 86 dB minimum, dc to 10 kHz
- Low offset voltage drift:  $\pm 2$   $\mu$ V/ $^{\circ}$ C maximum (B Grade)
- Low gain drift: 1 ppm/ $^{\circ}$ C maximum (B Grade)
- Enhanced slew rate: 1.1 V/ $\mu$ s
- Wide power supply range:
  - Single supply: 2 V to 36 V
  - Dual supplies:  $\pm 2$  V to  $\pm 18$  V

## APPLICATIONS

- Voltage measurement and monitoring
- Current measurement and monitoring
- Differential output instrumentation amplifier
- Portable, battery-powered equipment
- Test and measurement

## GENERAL DESCRIPTION

The AD8276/AD8277 are general-purpose, unity-gain difference amplifiers intended for precision signal conditioning in power critical applications that require both high performance and low power. They provide exceptional common-mode rejection ratio (86 dB) and high bandwidth while amplifying signals well beyond the supply rails. The on-chip resistors are laser-trimmed for excellent gain accuracy and high CMRR. They also have extremely low gain drift vs. temperature.

The common-mode range of the amplifiers extends to almost double the supply voltage, making these amplifiers ideal for single-supply applications that require a high common-mode voltage range. The internal resistors and ESD circuitry at the inputs also provide overvoltage protection to the op amps.

The AD8276/AD8277 are unity-gain stable. While they are optimized for use as difference amplifiers, they can also be connected in high precision, single-ended configurations with  $G = -1, +1, +2$ . The AD8276/AD8277 provide an integrated precision solution that has smaller size, lower cost, and better performance than a discrete alternative.

The AD8276/AD8277 operate on single supplies (2.0 V to 36 V) or dual supplies ( $\pm 2$  V to  $\pm 18$  V). The maximum quiescent supply current is 200  $\mu$ A per channel, which is ideal for battery-operated and portable systems.

Rev. C

Information furnished by Analog Devices is believed to be accurate and reliable. However, no responsibility is assumed by Analog Devices for its use, nor for any infringements of patents or other rights of third parties that may result from its use. Specifications subject to change without notice. No license is granted by implication or otherwise under any patent or patent rights of Analog Devices. Trademarks and registered trademarks are the property of their respective owners.

## FUNCTIONAL BLOCK DIAGRAM

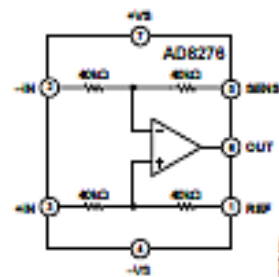


Figure 1. AD8276

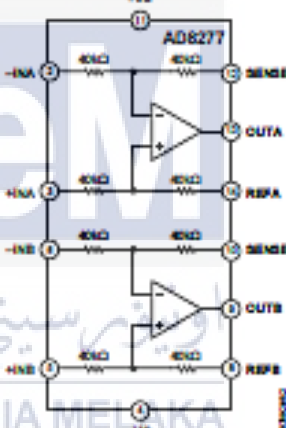


Figure 2. AD8277

Table 1. Difference Amplifiers by Category

Low Distortion	High Voltage	Current Sensing <sup>1</sup>	Low Power
AD8270	AD628	AD8202 (U)	AD8276
AD8271	AD629	AD8203 (U)	AD8277
AD8273		AD8205 (B)	AD8278
AD8274		AD8206 (B)	
AMP03		AD8216 (B)	

<sup>1</sup> U = unidirectional, B = bidirectional.

The AD8276 is available in the space-saving 8-lead MSOP and SOIC packages, and the AD8277 is offered in a 14-lead SOIC package. Both are specified for performance over the industrial temperature range of  $-40^{\circ}$ C to  $+85^{\circ}$ C and are fully RoHS compliant.

One Technology Way, P.O. Box 9106, Norwood, MA 02062-9106, U.S.A.  
Tel: 781.229.4700 [www.analog.com](http://www.analog.com)  
Fax: 781.461.2112 ©2009–2011 Analog Devices, Inc. All rights reserved.

## APPENDIX G



TLV3201, TLV3202

SBOS561B – MARCH 2012 – REVISED DECEMBER 2016

## TLV320x 40-ns, microPOWER, Push-Pull Output Comparators

### 1 Features

- Low Propagation Delay: 40 ns
- Low Quiescent Current:  
40  $\mu$ A per Channel
- Input Common-Mode Range Extends 200 mV  
Beyond Either Rail
- Low Input Offset Voltage: 1 mV
- Push-Pull Outputs
- Supply Range: 2.7 V to 5.5 V
- Industrial Temperature Range:  
–40°C to 125°C
- Small Packages:  
5-Pin SC70, 5-Pin SOT-23, 8-Pin SOIC, 8-Pin  
VSSOP

### 2 Applications

- Inspection Equipment
- Test and Measurement
- High-Speed Sampling Systems
- Teledom
- Portable Communications

### 3 Description

The TLV3201 and TLV3202 are single- and dual-channel comparators that offer the ultimate combination of high speed (40 ns) and low-power consumption (40  $\mu$ A), all in extremely small packages with features such as rail-to-rail inputs, low offset voltage (1 mV), and large output drive current. The devices are also very easy to implement in a wide variety of applications where response time is critical.

The TLV320x family is available in single (TLV3201) and dual (TLV3202) channel versions, both with push-pull outputs. The TLV3201 is available in 5-pin SOT-23 and 5-pin SC70 packages. The TLV3202 is available in 8-pin SOIC and 8-pin VSSOP packages. All devices are specified for operation across the expanded industrial temperature range of –40°C to 125°C.

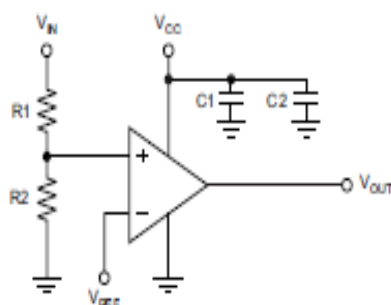
Device Information<sup>(1)</sup>

PART NUMBER	PACKAGE	BODY SIZE (NOM)
TLV3201	SOT-23 (5)	2.90 mm x 1.60 mm
	SC70 (5)	2.00 mm x 1.25 mm
TLV3202	VSSOP (8)	3.00 mm x 3.00 mm
	SOIC (8)	4.90 mm x 3.91 mm

(1) For all available packages, see the orderable addendum at the end of the data sheet.

UNIVERSITI TEKNIKAL MALAYSIA MELAKA

#### Threshold Detector



Copyright © 2016, Texas Instruments Incorporated